

Metallic surface of a Mott insulator—Mott insulating surface of a metal

M. Potthoff and W. Nolting

Institut für Physik, Humboldt-Universität zu Berlin, D-10115 Berlin, Germany

(Received 30 April 1999)

The dynamical mean-field theory (DMFT) is employed to study the correlation-driven metal-insulator transition in the semi-infinite Hubbard model at half-filling and zero temperature. We consider the low-index surfaces of the three-dimensional simple-cubic lattice, and systematically vary the model parameters at the very surface, the intralayer and interlayer surface hopping, and the surface Coulomb interaction. Within the DMFT the self-energy functional is assumed to be local. Therewith, the problem is self-consistently mapped onto a set of coupled effective impurity models corresponding to the inequivalent layers parallel to the surface. Assuming that the influence of the high-energy Hubbard bands on the low-energy quasiparticle resonance can be neglected at the critical point, a simplified “linearized DMFT” becomes possible. The linearized theory, however, is formally equivalent to the Weiss molecular-field theory for the semi-infinite Ising model. This implies that qualitatively the rich phenomenology of the Landau description of second-order phase transitions at surfaces has a direct analog for the surface Mott transition. Motivated by this formal analogy, we work out the predictions of the linearized DMFT in detail. It is found that under certain circumstances the surface of a Mott insulator can be metallic, while a Mott-insulating surface of a normal metal is not possible. We derive the corresponding phase diagrams, the (mean-field) critical exponents and the critical profiles of the quasiparticle weight. The results are confirmed by a fully numerical evaluation of the DMFT equations using the exact-diagonalization (ED) method. By means of the ED approach, we especially investigate the noncritical parts of the phase diagrams and discuss the U and layer dependence of the quasi-particle weight. For strong modifications of the surface model parameters, the surface low-energy electronic structure dynamically decouples from the bulk. [S0163-1829(99)10135-8]

I. INTRODUCTION

The correlation-driven transition from a paramagnetic metal to a paramagnetic Mott-Hubbard insulator^{1,2} constitutes one of the fundamental problems in solid-state theory. The Mott transition is interesting since strong electron correlations lead to low-energy electronic properties that are qualitatively different from those predicted by band theory.

Since it has been recognized that the limit of infinite spatial dimensions ($D=\infty$) is a well-defined and meaningful limit also for itinerant-electron models,³ and since the invention of dynamical mean-field theory (DMFT),^{4,5} there has been a renewed interest in the Mott transition.⁶ The DMFT provides an (in principle) exact description of the transition in infinite dimensions. While this is a somewhat artificial limit, the DMFT, as a mean-field concept, represents a powerful approach also for the study of finite-dimensional systems. Analogous to the Weiss molecular-field theory for localized spin models, the DMFT can be expected to give a valuable mean-field picture of the physics of three-dimensional itinerant-electron models.⁷

Presumably, the simplest model that includes the essentials of the Mott transition is the Hubbard model.^{8–10} From the application of the iterative perturbation theory (IPT)¹¹ to the $D=\infty$ Hubbard model at half-filling and zero temperature, the following scenario for the Mott transition has emerged:⁵ For small Coulomb interaction U , the system is a metallic Fermi liquid with a quasiparticle peak at the Fermi energy in the one-electron spectrum. As U approaches a critical value U_{c2} from below, the quasiparticle weight vanishes continuously, similar as in the Brinkman-Rice approach.¹²

For strong U the system is a Mott-Hubbard insulator with an insulating gap in the one-electron spectrum, similar to the Hubbard-III approach.¹³ The insulating solution ceases to exist when U approaches another critical value U_{c1} from above. In the entire coexistence region $U_{c1} < U < U_{c2}$ the metallic solution is stable, and thus the transition is of second order. The preformed gap opens discontinuously at $U_c = U_{c2}$.

It has been questioned^{14–17} whether the picture given by the IPT is correct. Recent numerical renormalization-group calculations (NRG),^{18,19} however, corroborate the IPT results qualitatively, although U_c is found to be significantly smaller than in the perturbational approach.²⁰ On the other hand, there is a remarkable agreement of the NRG with the result for U_c in the projective self-consistent method (PSCM).²¹

The NRG calculations show that, for $U \rightarrow U_c$, the quasiparticle resonance becomes more or less isolated from the high-energy Hubbard bands.¹⁹ The resonance basically reproduces itself in the self-consistent evaluation of the mean-field equations. This fact can be used for a simplified treatment of the DMFT where the influence of the Hubbard bands on the low-energy peak is neglected.²² This “linearized DMFT” yields a simple algebraic equation for the quasiparticle weight at the critical interaction, and thereby allows for an analytical estimate of U_c . The results are in good agreement with the numerical values for U_c obtained from NRG and PSCM on different lattices.²² For inhomogeneous systems, the linearized DMFT also determines the critical profile of the quasiparticle weight and the dependence of U_c on the system geometry. Comparing with the numerical results obtained from the exact diagonalization (ED) method, a con-

vincing qualitative agreement with respect to the thickness and geometry dependence of U_c has been found for thin Hubbard films.²³

It has been noticed²³ that the equation of the linearized DMFT is of the same form as the linearized mean-field equation of the Weiss molecular-field theory for the Ising model (at the critical temperature). There is a one-to-one correspondence if one identifies the quasiparticle weight z with the magnetization m , the squared interaction U^2 with the temperature T , and the squared hopping integral t^2 with the exchange coupling J :

$$z \Leftrightarrow m, \quad U^2 \Leftrightarrow k_B T, \quad 36t^2 \Leftrightarrow J/2. \quad (1)$$

The Weiss theory, on the other hand, can be considered as being a coarse-grained realization of the classical Landau theory of second-order phase transitions.²⁴ Consequently, the results of Landau theory (for $T=T_c$) can be translated back into predictions concerning the Mott transition in the Hubbard model (for $U=U_c$).

While the Landau theory of phase transitions is rather simple for homogeneous systems, the mean-field theory of critical behavior at *surfaces* is much more involved, and numerous nontrivial results can be derived.²⁵ The idea of the present paper is thus to take the Landau theory as starting point and motivation to work out the predictions of the linearized DMFT for Hubbard surfaces and finally to test the predictions, as far as possible, by comparing with a fully numerical solution of the DMFT equations.

Within the classical Landau theory, the free energy is expanded in terms of the local order parameter $m(\mathbf{r})$. For a semi-infinite system (surface geometry), one additionally considers a surface contribution to the free energy.²⁵ Laterally, the order parameter is assumed to be homogeneous. We take the x axis be parallel to the surface normal and pointing into the volume ($x>0$), then $m=m(x)$, and $m(x=0)$ is the surface value of the order parameter. Let us list those mean-field predictions derived from the Ginzburg-Landau free energy²⁵ which—by means of the above-mentioned formal analogy—have a direct counterpart for the Mott transition

(1) The transition in the bulk of the semi-infinite system occurs exactly at the same critical temperature $T_{c,\text{bulk}}$ as for the infinitely extended system: $T_{c,\text{bulk}}=T_c$.

(2) Near the surface, the order-parameter profile $m(x)$ vanishes at a distance Λ beyond the surface if linearly extrapolated from the boundary. The so-called ‘‘extrapolation length’’ Λ as well as the (bulk) correlation length ξ are the two length scales that characterize the order-parameter profile in the continuum model. Microscopically, the extrapolation length is related to the model parameters at the surface. In the molecular-field approximation of the Ising model we have $\Lambda^{-1} \propto (\Delta_c - \Delta)$, where Δ is the modification of the exchange coupling within the surface layer, $J_{11}=J(1+\Delta)$, and $\Delta=\Delta_c$ corresponds to $\Lambda=\infty$.

(3) For uniform parameters ($\Delta=0$) the mean field is smaller at the surface due to missing neighbors. This implies a weaker tendency to order. $m(x=0)$ is smaller than $m(x \rightarrow \infty)=m_{\text{bulk}}$, and $m(x)$ monotonously increases with increasing x (this implies $\Lambda>0$). There is a finite order parameter $m(x=0)>0$ at the surface only for $T<T_c$, i.e., only

when there is spontaneous order also in the bulk. The transition at T_c is termed the ‘‘ordinary transition.’’

(4) For $\Lambda<0$ ($\Delta>\Delta_c$) the surface layer orders at a temperature $T_{c,\text{surf}}>T_{c,\text{bulk}}$ (‘‘surface transition’’). In the regime $T_{c,\text{bulk}}<T<T_{c,\text{surf}}$, the bulk correlation length ξ is finite, and the order parameter decays exponentially fast from its maximum value $m(x=0)$ at the surface toward zero in the bulk. At $T=T_{c,\text{bulk}}$ (‘‘extraordinary transition’’), the divergence of ξ and the onset of order in the bulk induce singularities in the behavior of surface response functions. For the order parameter at the surface $m(x=0)$, there is a discontinuity of its second derivative only. At $T=T_{c,\text{bulk}}$ the order-parameter profile decays algebraically, $m(x) \propto 1/x$.

(5) It holds that $(T_{c,\text{surf}}-T_{c,\text{bulk}})/T_{c,\text{bulk}} \propto \Lambda^{-2}$. The transition at $T=T_{c,\text{surf}}=T_{c,\text{bulk}}$ in the case $\Lambda=\infty$ is called the ‘‘special transition.’’ For $\Lambda=\infty$ the order-parameter profile is flat in the ordered phase; the trivial solution $m(x)=m_{\text{bulk}}=\text{const}$ minimizes the Ginzburg-Landau free energy. In this situation the effect of missing neighbors at the surface is compensated for exactly. The topology of the phase diagram (ordinary, extraordinary, surface, and special transition) should be correct *whenever* the surface can support independent order.²⁶ For example, there is no surface transition in the semi-infinite two-dimensional Ising model since the ‘‘surface’’ is one dimensional.²⁷

(6) There are two critical exponents that are merely related to the critical temperatures (instead of describing the critical behavior of order parameter and response functions), the ‘‘shift exponent’’ λ_s , and the ‘‘crossover exponent’’ ϕ . They are defined as $[T_c(d)-T_c(d=\infty)]/T_c(d=\infty) \propto d^{-\lambda_s}$ for $d \rightarrow \infty$, where $T_c(d)$ is the critical temperature of a film of finite thickness d , and $[T_{c,\text{surf}}(\Delta)-T_{c,\text{bulk}}]/T_{c,\text{bulk}} \propto (\Delta/\Delta_c - 1)^{1/\phi}$ for $\Delta \rightarrow \Delta_c$ (special transition). Within Landau mean-field theory one has $\lambda_s=2$ and $\phi=1/2$.

(7) Spontaneous order in the bulk always induces a finite order parameter at the surface, $m(x=0)>0$.

The Landau theory also makes additional statements concerning, e.g., the bulk and surface critical exponents of the order parameter as well as the exponents of response functions with respect to an external applied field. We do not mention such results in the present context, since either they have no obvious analog for the Mott transition (applied field) or they refer to temperatures $T \rightarrow T_c$ but $T \neq T_c$ where the mean-field equation cannot be linearized and where the formal analogy [Eq. (1)] breaks down. We will, however, discuss a simple extension of the linearized DMFT for $U \rightarrow U_c$ but $U \neq U_c$ which recovers the result $z \propto (U_c - U)$ of the PSCM.²¹

To a certain extent, the phase diagram predicted by the Landau theory or, respectively, by the linearized DMFT can be tested by comparing with a fully numerical evaluation of the DMFT equations. We need an approach that is sufficiently simple for a systematic study of a large number of geometries and model parameters. For this purpose the exact-diagonalization method of Caffarel and Krauth²⁸ is well suited. We mainly focus on the noncritical parts in the phase diagram where the ED is able to give reliable results. Critical exponents, for example, cannot be calculated reliably. The ED has successfully been employed beforehand for the discussion of the Mott transition in thin Hubbard films²³ and at Hubbard surfaces,²⁹ where the film and surface elec-

tronic structure has been discussed in detail. Conversely, the present paper focuses on the surface modification of the model parameters and on surface phases, and thereby substantially extends the previous studies.

The Mott transition at a surface of the semi-infinite Hubbard model has recently been investigated in a paper by Hasegawa³⁰ on the basis of the Kotliar-Ruckenstein slave-boson theory.³¹ With the present study we methodically improve upon Hasegawa's work. We will also show that for $U \mapsto U_c$ the perturbation of the system that is introduced by the presence of the surface deeply extends into the bulk. It is thus insufficient to assume (local) physical quantities to be different from their value in the bulk only in the first few surface layers. Such a restriction gives rise to unphysical singularities, e.g., in the U dependence of the quasiparticle weight, as they are seen in Ref. 30. Within the slave-boson theory it is found that under certain circumstances a metallic surface can coexist with an insulating bulk.³⁰ Crucial for the existence of this surface phase is a considerable decrease of U at the surface. This is an interesting and also plausible result, although the required strong decrease of U at the surface appears to be quite unrealistic for real systems.

A physically more relevant modification of the model parameters is, in the first place, the enhancement or decrease of the hopping integrals at the surface. This may be caused by a relaxation of the interlayer distance, for example. According to the scaling law $t \sim r^{-5}$ for d electrons (cf., e.g., Ref. 32), a top-layer relaxation $\Delta r/r$ of a few percent results in a strong change of the hopping integral. A surface modification of t up to about 10–20% appears to be realistic. Besides the hopping we will also discuss a modification of U at the surface. In $3d$ transition metals, however, this effect seems to be less important.^{33,34} In any case, U is expected to be enhanced at the surface.³⁴ On the contrary, it will be shown that the interesting surface phase occurs for *lowered* surface U . Another important aspect is the surface geometry which is expected to affect the surface phase diagram considerably. Open surfaces with a strong reduction of the surface coordination number will show the most pronounced surface effects in the electronic structure. We thus consider different low-index surfaces of a $D=3$ simple-cubic (sc) lattice.

The basic assumption of DMFT is the strict locality of the self-energy functional. For $D=3$ dimensions this represents a strong simplification of the problem. The local approximation is well justified for the weak-coupling regime, and also for the case of surface geometries (see the discussion in Refs. 29, 35, and 36). For the intermediate- to strong-coupling regime, however, the assumption may be questioned. One could alternatively investigate a surface of a $D=\infty$ lattice where the DMFT becomes exact. While this will be discussed briefly, we otherwise consider surfaces in $D=3$ dimensions. As in Refs. 23 and 29, we expect the mean-field concept to be a good starting point for $D=3$.

The plan of this paper is the following: Section II introduces the model. The application of DMFT for surface geometries is briefly discussed in Sec. III. We use two different methods to solve the DMFT equations: The first one is an approximative linearization of the equations for $U=U_c$.²² This is presented in Sec. IV. Section V then gives a discussion of the analytical results. For the full solution of the DMFT equations, we employ the exact-diagonalization

method²⁸ which is introduced in Sec. VI. The corresponding results are discussed in Sec. VII. Finally, Sec. VIII concludes the paper.

II. SEMI-INFINITE HUBBARD MODEL

We investigate the Hubbard model on a three-dimensional, simple-cubic, and semiinfinite lattice. The system is considered to be built up by two-dimensional layers parallel to the surface. Accordingly, the position vector to a particular site in the semi-infinite lattice is written as $\mathbf{R}_{\text{site}} = \mathbf{r}_i + \mathbf{R}_\alpha$. Here \mathbf{R}_α stands for the coordinate origin in the layer α , and the layer index runs from $\alpha=1$ (topmost surface layer) to infinity (bulk). \mathbf{r}_i is the position vector with respect to a layer-dependent origin, and runs over the sites within the layer. In this notation, the Hamiltonian reads

$$H = \sum_{ij\alpha\beta\sigma} t_{i\alpha,j\beta} c_{i\alpha\sigma}^\dagger c_{j\beta\sigma} + \sum_{i\alpha\sigma} \frac{U_\alpha}{2} n_{i\alpha\sigma} n_{i\alpha-\sigma}. \quad (2)$$

$\sigma = \uparrow, \downarrow$ is the spin index. U_α is the (layer-dependent) Hubbard interaction strength. The hopping integrals are restricted to be nonzero between nearest neighbors. The energy zero is defined by setting $t_{i\alpha,i\alpha} \equiv t_0 = 0$ for sites in the bulk ($\alpha \rightarrow \infty$). The energy scale is given by taking the (bulk) nearest-neighbor hopping to be $t_{\langle i\alpha,j\beta \rangle} = -t$ with $t=1$.

The presence of the surface implies a breakdown of translational symmetry with respect to the surface normal direction. Lateral translational symmetry, however, may be exploited by performing a two-dimensional Fourier transformation

$$\epsilon_{\alpha\beta}(\mathbf{k}) = \frac{1}{N_\parallel} \sum_{ij} e^{-i\mathbf{k}(\mathbf{r}_i - \mathbf{r}_j)} t_{i\alpha,j\beta}. \quad (3)$$

Here \mathbf{k} is a two-dimensional wave vector of the first surface Brillouin zone, and N_\parallel denotes the number of sites within each layer ($N_\parallel \rightarrow \infty$). Let us briefly discuss the Fourier-transformed hopping matrix, which reads

$$\epsilon(\mathbf{k}) = \begin{pmatrix} t_{11}\epsilon_\parallel(\mathbf{k}) + \Delta t_0 & t_{12}\epsilon_\perp(\mathbf{k}) & & & \\ t_{21}\epsilon_\perp(\mathbf{k}) & t\epsilon_\parallel(\mathbf{k}) & t\epsilon_\perp(\mathbf{k}) & & \\ & t\epsilon_\perp(\mathbf{k}) & t\epsilon_\parallel(\mathbf{k}) & \dots & \\ & & \dots & \dots & \dots \end{pmatrix}. \quad (4)$$

For $\alpha \geq 2$, the intralayer (parallel) hopping and the interlayer (perpendicular) hopping are written as $\epsilon_{\alpha\alpha}(\mathbf{k}) = t\epsilon_\parallel(\mathbf{k})$ and $\epsilon_{\alpha\alpha+1}(\mathbf{k}) = t\epsilon_\perp(\mathbf{k})$, respectively. We consider three different low-index surfaces of the sc lattice. The hopping matrix for the sc(100) surface is obtained from

$$\epsilon_\parallel(\mathbf{k}) = -2[\cos(k_x) + \cos(k_y)], \quad |\epsilon_\perp(\mathbf{k})|^2 = 1. \quad (5)$$

The perpendicular hopping is \mathbf{k} independent in this case. For the (110) surface, we have

$$\epsilon_\parallel(\mathbf{k}) = -2\cos(k_x), \quad |\epsilon_\perp(\mathbf{k})|^2 = 2 + 2\cos(\sqrt{2}k_y), \quad (6)$$

and, for the sc(111) surface,

$$\epsilon_{\parallel}(\mathbf{k})=0, \quad (7)$$

$$|\epsilon_{\perp}(\mathbf{k})|^2=3+2\cos(\sqrt{2}k_y)+4\cos(\sqrt{3/2}k_x)\cos(\sqrt{1/2}k_y).$$

Since two nearest neighbors are always located in two different (adjacent) layer, the intralayer hopping vanishes in the last case. Note that only the absolute square of $\epsilon_{\perp}(\mathbf{k})$ enters the physical quantities we are interested in.

At the very surface of the semi-infinite system, we consider three different possible modifications of the model parameters. First, the intralayer hopping within the topmost surface layer t_{11} may differ from its bulk value [see Eq. (4)]. Second, we allow for an altered hopping $t_{12}=t_{21}\neq t$ between the topmost and the first subsurface layer. Finally, the on-site Coulomb interaction strength is assumed to be layer independent, $U_{\alpha}=U=\text{const}$, except for the topmost layer $U_{\alpha=1}\neq U$.

We restrict ourselves to the case of manifest particle-hole symmetry, namely, a bipartite (sc) lattice, nearest-neighbor hopping and half-filling ($n=2\langle n_{i\alpha\sigma}\rangle=1$). In this case the Fermi energy is given by $\mu=t_0+U/2$. It is fixed by the bulk values for the on-site hopping and for the Hubbard interaction. Consider the atomic limit $t=0$ for a moment: The positions of the two Hubbard ‘‘bands’’ in the bulk spectrum are given by $E_{\text{low}}=t_0-\mu$ and $E_{\text{high}}=t_0-\mu+U$, i.e., they lie *symmetric* with respect to μ . In thermal equilibrium, μ is also the Fermi energy for the top layer. The Hubbard peaks in the surface density of states lie at $E_{\text{low}}=t_0-\mu+\Delta t_0$ and $E_{\text{high}}=t_0+\Delta t_0-\mu+U_1$, where we have taken into account the top-layer modification of the interaction strength and where we have introduced an additional modification Δt_0 of the atomic level for top-layer sites [see Eq. (4)]. To maintain manifest particle-hole symmetry and to ensure $\langle n_{i\alpha\sigma}\rangle=0.5$ for $\alpha=1$, the Hubbard peaks must again lie symmetric with respect to μ . Thus we need

$$\Delta t_0=(U-U_1)/2. \quad (8)$$

With this choice for the top-layer on-site hopping, the local density of states $\rho_{\alpha}(E)=(-1/\pi)\text{Im}\langle\langle c_{i\alpha\sigma};c_{i\alpha\sigma}^{\dagger}\rangle\rangle_E$ is a symmetric function of energy for each α .

We finally introduce the intralayer and interlayer coordination numbers q and p which denote the number of nearest neighbors within the same layer and in one of the two adjacent layers, respectively. We have

$$\begin{aligned} q=4, \quad p=1 & \text{ for sc(100),} \\ q=2, \quad p=2 & \text{ for sc(110),} \\ q=0, \quad p=3 & \text{ for sc(111).} \end{aligned} \quad (9)$$

The bulk coordination number is $Z=q+2p$. The surface coordination number is $Z_S=q+p$.

III. DYNAMICAL MEAN-FIELD THEORY FOR SURFACE GEOMETRIES

The one-particle Green function $\langle\langle c_{i\alpha\sigma};c_{j\beta\sigma}^{\dagger}\rangle\rangle$ contains any important information we are interested in. Its diagonal elements $G_{\alpha}(E)\equiv G_{i\alpha,i\alpha}(E)\equiv\langle\langle c_{i\alpha\sigma};c_{i\alpha\sigma}^{\dagger}\rangle\rangle_E$ can be written in terms of the hopping matrix (4) and the self-energy

$$G_{\alpha}(E)=\frac{1}{N_{\parallel}}\sum_{\mathbf{k}}\left(\frac{1}{(E+\mu)\mathbf{1}-\epsilon(\mathbf{k})-\Sigma(E)}\right)_{\alpha\alpha}. \quad (10)$$

The self-energy matrix is taken to be \mathbf{k} independent and diagonal, $\Sigma_{\alpha\beta}(E)=\delta_{\alpha\beta}\Sigma_{\alpha}(E)$, with layer-dependent elements: We assume that the self-energy is a strictly *local* quantity.

In the case of an infinitely extended lattice with full translational symmetry, this basic assumption leads to the well-known equations of dynamical mean-field theory^{4,5} which self-consistently map the bulk lattice problem onto a single-impurity problem.^{11,37} The present case of reduced translational symmetry can be treated analogously: A local self-energy implies that the Luttinger-Ward functional³⁸ depends on the local (but layer-dependent) propagators only: $\Phi=\Phi[\dots,G_{\alpha}(E),\dots]$. This in turn means that the self-energy of the α th layer is solely a functional of the local propagator: $\Sigma_{\alpha}(E)=\delta\Phi/\delta G_{\alpha}(E)=\mathcal{S}[G_{\alpha}(E)]$. The functional \mathcal{S} is the same as in the case of an impurity problem, e.g., the single-impurity Anderson model (SIAM), $\Sigma_{\text{imp}}(E)=\mathcal{S}[G_{\text{imp}}(E)]$, because the same type of skeleton diagrams occur in the expansion of the impurity self-energy $\Sigma_{\text{imp}}(E)$. With each layer $\alpha=1,2,\dots$ we therefore associate a SIAM,

$$\begin{aligned} H_{\text{imp}}^{(\alpha)}&=\sum_{\sigma}\epsilon_d^{(\alpha)}c_{\sigma}^{\dagger}c_{\sigma}+U_{\alpha}n_{\uparrow}n_{\downarrow}+\sum_{k\sigma}\epsilon_k^{(\alpha)}a_{k\sigma}^{\dagger}a_{k\sigma} \\ &+\sum_{k\sigma}(V_k^{(\alpha)}a_{k\sigma}^{\dagger}c_{\sigma}+\text{H.c.}), \end{aligned} \quad (11)$$

with $\epsilon_d^{(\alpha)}=t_{i\alpha,i\alpha}$ and where the conduction-band energies $\epsilon_k^{(\alpha)}$ and hybridization strengths $V_k^{(\alpha)}$ chosen such that we have

$$\Delta^{(\alpha)}(E)=E+\mu-\epsilon_d^{(\alpha)}-\Sigma_{\text{imp}}^{(\alpha)}(E)-G_{\alpha}(E)^{-1} \quad (12)$$

for the hybridization function $\Delta^{(\alpha)}(E-\mu)\equiv\sum_k(V_k^{(\alpha)})^2/(E-\epsilon_k^{(\alpha)})$. [Eq. (12) only provides an implicit definition of the hybridization function since $\Sigma_{\text{imp}}^{(\alpha)}$ depends on $\Delta^{(\alpha)}$]. This implies at once the equality between the impurity Green function of the α th SIAM, $G_{\text{imp}}^{(\alpha)}(E)$, and the on-site lattice Green function in the α th layer $G_{\alpha}(E)$ and thus the equality between the respective self-energies, $\Sigma_{\text{imp}}^{(\alpha)}(E)=\mathcal{S}[G_{\text{imp}}^{(\alpha)}(E)]$ and $\Sigma_{\alpha}(E)=\mathcal{S}[G_{\alpha}(E)]$.

The following iterative procedure then allows to solve the semi-infinite Hubbard model within the dynamical mean-field approximation: Starting from a guess for the layer-dependent self-energies $\Sigma_{\alpha}(E)$, we calculate the on-site Green function of the α th layer using Eq. (10). Via Eq. (12), $G_{\alpha}(E)$ and $\Sigma_{\alpha}(E)=\Sigma_{\text{imp}}^{(\alpha)}(E)$ determine the hybridization function $\Delta^{(\alpha)}(E)$ of the α th SIAM. The crucial step consists of solving the impurity models for $\alpha=1,2,\dots$ to obtain the impurity self-energies $\Sigma_{\text{imp}}^{(\alpha)}(E)$ which are required for the next cycle. The cycles have to be repeated until self-consistency is achieved.

Applying the DMFT to the semi-infinite Hubbard model means mapping the original lattice problem onto an infinite set of impurity problems. The mapping is mediated by the self-consistency equation (12) for $\alpha=1,2,\dots,\infty$. For a given set of hybridization functions, each impurity model can be treated separately. There is, however, an indirect cou-

pling via Eq. (10) in the self-consistency cycle since the on-site Green function of a given layer depends on all layer-dependent self-energies. The essential difference with respect to the case of an infinitely extended lattice with full translational symmetry where only one single-impurity model and only one self-consistency condition is needed, consists of the fact that, for a semi-infinite system, the sites within different layers have to be considered as nonequivalent.

IV. LINEARIZED DMFT AT THE CRITICAL INTERACTION

The zero-temperature Mott transition from a paramagnetic metal to a paramagnetic insulator is actually hidden due to antiferromagnetic order which is realized in the true ground state. To study the Mott transition, the solutions of the mean-field equations have to be enforced to be spin symmetric. There have been numerous DMFT studies of the $T=0$ Mott transition in the recent past using different methods to solve the impurity problem: the iterative perturbation theory (IPT),^{11,39,40} the ED approach,^{28,41,42} the projective self-consistent method,²¹ and numerical renormalization-group calculations.^{18,19}

The IPT and, in first place, the NRG results show that for $U \mapsto U_c$ the quasiparticle resonance at $E=0$ is more or less isolated from the high-energy Hubbard peaks at $E \approx \pm U/2$. The resonance basically reproduces itself in the self-consistent procedure to solve the DMFT equations. A reasonable assumption is therefore that for $U=U_c$ the low-energy part of the SIAM hybridization function $\Delta^{(\alpha)}(E)$ consists of a single pole at $E=0$ only,

$$\Delta^{(\alpha)}(E) \mapsto \frac{\Delta_N^{(\alpha)}}{E}, \quad (13)$$

and that the effect of the Hubbard bands can be disregarded completely. With this assumption a simplified, ‘‘linearized’’ DMFT becomes possible.^{22,23} There is an attractive feature of this method which outweighs the necessity for a further approximation: It allows for a fully analytic treatment of the mean-field equations, and an analytical expression for U_c is obtained. Studying the dependencies of U_c on the model parameters can provide a valuable first insight into the problem. The predictions of the linearized theory have been compared beforehand with fully numerical DMFT results for the Bethe and the hypercubic lattice in $D=\infty$,²² and for the case of thin Hubbard films.²³ A satisfactory quantitative agreement has been noticed. This makes us confident that at least the correct trends can also be predicted for the case of a semi-infinite lattice.

The details of the method can be found in Ref. 22; here we simply repeat the main idea and the final result: In the ansatz for the hybridization function (13), $\Delta_N^{(\alpha)}$ denotes the layer-dependent coefficient in the N th step of the self-consistency cycle. The aim is to calculate $\Delta_{N+1}^{(\alpha)}$. The one-pole structure of the hybridization function corresponds to a well-defined SIAM with $n_s=2$ sites which can analytically be solved for each α . In the one-particle excitation spectrum of the α th SIAM, there are two δ peaks at $E \approx \pm U_\alpha/2$ as well as two δ peaks near $E=0$ corresponding to the (infi-

nately sharp) Kondo resonance for $U=U_c$ in the infinite ($n_s=\infty$) system. The layer-dependent weight of the resonance z_α can be read off from the solution. z_α determines the self-energy $\Sigma_\alpha(E) = U_\alpha/2 + (1-z_\alpha^{-1})E + \dots$, and via Eq. (10) the on-site Green function of the α th layer at low energies. Using these results in the self-consistency equation (12) and insisting on the one-pole structure of the hybridization function, yields a new coefficient $\Delta_{N+1}^{(\alpha)}$. At this point the possible influence of the Hubbard bands is ignored. The final equation that relates $\Delta_{N+1}^{(\alpha)}$ to $\Delta_N^{(\alpha)}$ reads

$$\Delta_{N+1}^{(\alpha)} = \sum_{\beta} K_{\alpha\beta} \Delta_N^{(\beta)}, \quad (14)$$

where we have defined the following semi-infinite tridiagonal matrix:

$$\mathbf{K} = 36 \begin{pmatrix} qt_{11}^2/U_1^2 & pt_{12}t/U_1U & & & & \\ pt_{12}t/U_1U & qt^2/U^2 & p t^2/U^2 & & & \\ & pt^2/U^2 & qt^2/U^2 & \dots & & \\ & & & \dots & \dots & \\ & & & & \dots & \dots \end{pmatrix}. \quad (15)$$

A self-consistent solution of the linearized mean-field equation (14) is given by a nontrivial fixed point of \mathbf{K} . Let λ_r denote the eigenvalues of \mathbf{K} . We can distinguish between two cases: If $|\lambda_r| < 1$ for all r , there is the trivial solution $\lim_{N \rightarrow \infty} \Delta_N^{(\alpha)} = 0$ only. This situation corresponds to the insulating solution beyond the critical point. Conversely, if there is at least one $\lambda_r > 1$, $\Delta_N^{(\alpha)}$ diverges exponentially as $N \rightarrow \infty$. This indicates the breakdown of the one-pole model for the hybridization function in the metallic solution below the critical point. The maximum eigenvalue thus determines, via

$$\lambda_{\max} = \lambda_{\max}(q, p, U, t_{11}, t_{12}, U_1) = 1, \quad (16)$$

the critical model parameters.

At the critical point the mean-field equation (14) can be written as $z_\alpha = \sum_{\beta} K_{\alpha\beta} z_\beta$ since the layer-dependent quasiparticle weight $z_\alpha \propto \Delta^{(\alpha)}$. Formally, this equation can be compared with the Weiss mean-field equation for the layer magnetizations m_α in the semi-infinite Ising model with coupling constant J . The linearized mean-field equation for $T=T_C$ reads $m_\alpha = (J/2k_B T)(qm_\alpha + pm_{\alpha+1} + pm_{\alpha-1})$ (we assume the model parameters at the surface to be unmodified for the moment). The formal analogy with Eqs. (14) and (15) is obvious and justifies the identification made in Eq. (1) and the corresponding discussion in Sec. I.

V. ANALYTICAL RESULTS

From the basic equation (16) we can calculate the critical parameters for different cases. First, we consider a system that is built up by a finite number of d layers (film geometry). The model parameters are taken to be *uniform*, i.e., $t_{11}=t_{12}=t$ and $U_1=U$ (at both surfaces). The eigenvalues of the d -dimensional matrix (15) can be calculated analytically for this case,⁴³

$$\lambda_r = \frac{36t^2}{U^2} \left[q + 2p \cos\left(\frac{r\pi}{d+1}\right) \right], \quad (17)$$

with $r = 1, \dots, d$. Taking the maximum eigenvalue and solving for U yields the thickness dependence of the critical interaction²³

$$U_c(d) = 6t \sqrt{q + 2p \cos\left(\frac{\pi}{d+1}\right)}. \quad (18)$$

Expanding the result for U_c in the limit of $d \rightarrow \infty$ yields

$$\frac{U_c(d) - U_c(\infty)}{U_c(\infty)} \propto d^{-\lambda_s}, \quad (19)$$

with a ‘‘shift exponent’’ $\lambda_s = 2$.

In the limit $d = \infty$ any of the two film surfaces represents a semi-infinite system. From Eq. (18) we obtain, for the critical interaction,

$$U_{c,\text{bulk}} = 6t \sqrt{q + 2p} = 6t \sqrt{Z}, \quad (20)$$

which is the same result as is found when applying the method to the infinitely extended bulk system directly.²² We notice that for the case of uniform model parameters the linearized DMFT yields a unique critical interaction for the semi-infinite system which is the same as the bulk value. No surface phase is found. This observation is fully consistent with what has been obtained in previous numerical DMFT studies of the Mott transition at Hubbard surfaces²⁹ for *uniform* parameters. Despite the fact that at the surface the electronic structure has turned out to be modified considerably, a surface critical interaction different from the bulk value has not been found.

In the following we thus concentrate on a semi-infinite system with *modified* parameters at the very surface. Also in this case, condition (16) can be treated analytically: To simplify the notation let us write $K_{11} = a'$, $K_{12} = K_{21} = b'$ and $K_{\alpha\alpha} = a$, $K_{\alpha\alpha\pm 1} = b$ for $\alpha \geq 2$ ($a, b, a', b' \geq 0$). Let $\mathbf{K}(n)$ be the matrix that is obtained from the semi-infinite matrix $\mathbf{K} = \mathbf{K}(0)$ by deleting its first n rows and columns. Furthermore, we define $\mathcal{G}_n(\lambda) \equiv \det[\lambda \mathbf{1} - \mathbf{K}(n+1)] / \det[\lambda \mathbf{1} - \mathbf{K}(n)]$. $\mathcal{G}_n(\lambda)$ is the (1,1) or ‘‘surface’’ element of the Green matrix $[\lambda \mathbf{1} - \mathbf{K}(n)]^{-1}$. Expanding the determinant $\det[\lambda \mathbf{1} - \mathbf{K}(n+1)]$ with respect to the upper left element, one easily verifies the recurrence relation $\mathcal{G}_n(\lambda)^{-1} = \lambda - a - b^2 \mathcal{G}_{n+1}(\lambda)$ for $n \geq 1$. However, all the $\mathcal{G}_n(\lambda)$ for $n \geq 1$ must be equal since the (off-)diagonal elements of $\mathbf{K}(n \geq 1)$ are constant. This results in a quadratic equation for \mathcal{G} , the solution of which is given by

$$\mathcal{G}(\lambda) = \mathcal{G}_{n \geq 1}(\lambda) = \frac{1}{2b^2} [(\lambda - a \mp \sqrt{(\lambda - a)^2 - 4b^2})] \quad (21)$$

for $\pm(\lambda - a) > 0$. The eigenvalue spectrum of the semi-infinite matrix \mathbf{K} consists of a continuous bulk part which can be read off from Eq. (17) for $d \rightarrow \infty$ to be given by

$$|\lambda - a| \leq 2b. \quad (22)$$

This is just the region where $\text{Im} \mathcal{G}(\lambda) \neq 0$. The largest eigenvalue in the bulk continuum is given by $\lambda = a + 2b$, corresponding to the bulk critical interaction given in Eq. (20). At

$U = U_{c,\text{bulk}}$ the bulk undergoes the metal-insulator transition irrespective of the state of the surface.

Under certain circumstances an additional discrete (‘‘surface’’) eigenvalue λ_s may split off the bulk continuum. If a discrete eigenvalue exists, we must have $\mathcal{G}_0(\lambda_s)^{-1} = 0$. Using the result (21) to determine $\mathcal{G}_0(\lambda)$ from the recurrence relation $\mathcal{G}_0(\lambda)^{-1} = \lambda - a' - b'^2 \mathcal{G}(\lambda)$, we obtain the following equation for the eigenvalue:

$$\lambda_s - a' - b'^2 \left[\frac{1}{2b^2} (\lambda_s - a \mp \sqrt{(\lambda_s - a)^2 - 4b^2}) \right] = 0 \quad (23)$$

[$\pm(\lambda_s - a) > 0$]. Solving the equation for λ_s yields the position of the eigenvalue in the spectrum of \mathbf{K} . Since \mathbf{K} is real and symmetric, only a solution λ_s with $\text{Im} \lambda_s = 0$ is meaningful; a discrete λ_s must lie outside the bulk continuum (22). Only the maximum eigenvalue in the spectrum is physically relevant [Eq. (16)]. Thus we are interested in a solution that is split off the upper edge of the continuum:

$$\text{Re} \lambda_s > a + 2b. \quad (24)$$

Since $b \geq 0$ only the $-$ sign must be considered in Eq. (23).

Whether or not condition (24) can be met depends on the (surface) parameters a' and b' . Solving Eq. (23) for λ_s and inserting the solution into Eq. (24), yields the following relation for a' and b' :

$$2b^2 + b(a - a') - b'^2 < 0, \quad (25)$$

which must be fulfilled to obtain a (physically relevant) surface mode. Note that the relation cannot be satisfied with uniform parameters, i.e., $a' = a$ and $b' = b$.

The interpretation is the following: In a semi-infinite system with surface parameters t_{11} , t_{12} , and U_1 that do not obey condition (25), there is only the ‘‘ordinary’’ transition from a metallic to a Mott insulating state at $U = U_{c,\text{bulk}}$ when increasing the interaction strength. The critical interaction $U_{c,\text{bulk}}$ is given by Eq. (20). At this point all layer-dependent quasiparticle weights z_α , in the bulk as well as at the surface, vanish. On the other hand, for a sufficiently strong modification of t_{11} , t_{12} , or U_1 , i.e., for a' and b' satisfying Eq. (25), there are *two* critical interaction strengths: The first one is $U_{c,\text{bulk}}$ again. At $U = U_{c,\text{bulk}}$ the bulk quasiparticle weight $z_{\alpha=\infty}$ vanishes. The second critical interaction strength $U_{c,\text{surf}}$ can be determined from $\lambda_s \stackrel{!}{=} 1$ where λ_s is the solution of Eq. (23). Let us assume that $U_{c,\text{surf}} > U_{c,\text{bulk}}$. For $U > U_{c,\text{surf}}$ the entire system is in the Mott insulating phase. For $U_{c,\text{bulk}} < U < U_{c,\text{surf}}$, however, the bulk is a Mott insulator while the surface is still metallic. We call the transition at $U = U_{c,\text{bulk}}$ the ‘‘extraordinary’’ and the transition at $U = U_{c,\text{surf}}$ the ‘‘surface transition’’ in analogy with the terminology for magnetic phase transitions at surfaces.²⁵

The remaining question is whether or not $U_{c,\text{surf}} < U_{c,\text{bulk}}$ can be possible. In such a situation we would have a quasi-two-dimensional Mott insulator on top of a metallic bulk for interactions $U_{c,\text{surf}} < U < U_{c,\text{bulk}}$. However, this possibility is ruled out: Eq. (24) can be rewritten as $\lambda_s > U_{c,\text{bulk}}^2 / U^2$. Furthermore, at the critical point $U = U_{c,\text{surf}}$ the value $\lambda_s = 1$ fulfills Eq. (23). But this implies $1 > U_{c,\text{bulk}}^2 / U_{c,\text{surf}}^2$. We can state that the linearized theory predicts that a metallic surface

coexisting with a Mott insulating bulk is possible while the opposite scenario cannot be realized.

Arguing physically, if (at the Fermi edge) there is a finite (local) density of states in the second and all subsequent layers, this must always induce a nonzero, though possibly low density of states in the top layer, and thus an insulating surface phase is excluded: Consider the free-standing two-dimensional layer at an interaction strength U_1 being sufficiently strong to force the system to the insulating phase. Let the monolayer be coupled to the second and all subsequent layers by switching on the hopping between the top layer and the second layer $t_{12} \neq 0$. If t_{12} is finite but too small, the low-energy bulk excitations cannot propagate into the top layer and are reflected at the Hubbard gap. However, virtual hopping processes are possible which cause (an exponentially damped) weight of bulk excitations in the top layer. The exponential damping becomes unimportant in this case, since it is effective in one layer only.

For the opposite case of a metallic surface on top of a Mott insulator, however, it does become essential: Low-energy excitations can propagate within the surface region since $U < U_{c,\text{surf}}$. Because $U > U_{c,\text{bulk}}$, they cannot propagate into the bulk but are reflected at the (bulk) Hubbard gap. While virtual processes always generate some nonzero spectral weight at the Fermi edge in each layer, the weight is infinitesimally small asymptotically, for $\alpha \rightarrow \infty$.

Since critical fluctuations spread out all over the system at a second-order critical point, different parts of a system should undergo the transition at a common and unique critical value of the external control parameter. The exponential damping of low-energy excitations over large distances explains why there can be *two* critical interactions. This is analogous to the case of magnetic phase transitions at surfaces: In a system where a magnetic surface coexists with a paramagnetic bulk, the layer magnetization must decay exponentially when passing from the surface to the crystal volume. Conversely, a magnetic bulk always induces a finite magnetization in the top layer. The exception is the somehow artificial case where the top layer is completely decoupled from the rest system (e.g., $t_{12} = 0$).

A. Modified intralayer surface hopping

Some more aspects of the metallic surface phase shall be addressed in the following. In particular, to discuss the effects of the surface geometry, we refer to the different low-index surfaces of the sc lattice mentioned above. Furthermore, it is helpful to consider the different types of surface modifications separately.

We start by considering a modified intralayer hopping in the top layer: $t_{11} \neq t$. We have

$$a' = \frac{t_{11}^2}{t^2} a, \quad b' = b. \quad (26)$$

From Eq. (25) we can deduce that there are two critical interactions, provided that

$$t_{11} > t \sqrt{1 + \frac{p}{q}}. \quad (27)$$

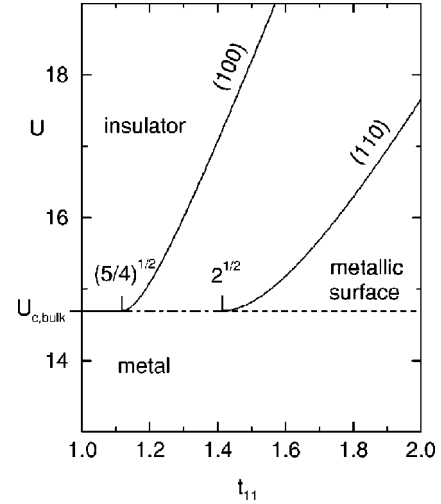


FIG. 1. t_{11} - U phase diagram as obtained from the linearized DMFT. For $U < U_{c,\text{bulk}}$, the system is metallic. For $U > U_{c,\text{bulk}}$ the bulk is a Mott insulator, and the surface can be either insulating (left to the phase boundary) or metallic (right). Phase boundaries for the (100) and (110) surfaces of the sc lattice. Energy units: nearest-neighbor hopping $t = 1$. Free bandwidth $W = 12$.

According to Eq. (16) and (23), the critical interaction strength at which the surface transition takes place, is given by

$$U_{c,\text{surf}} = 6t \sqrt{q \frac{t_{11}^2}{t^2} + \frac{p^2}{q} \frac{t^2}{t_{11}^2 - t^2}}. \quad (28)$$

The corresponding phase diagram is shown in Fig. 1.

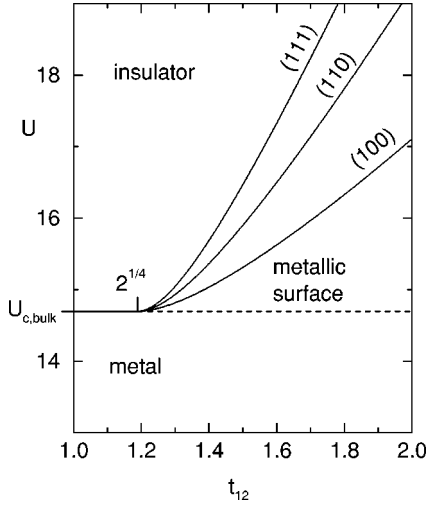
For the (111) surface there is no intralayer hopping at all ($q = 0$). A rather moderate enhancement of t_{11} (about 12%) is sufficient to obtain a metallic surface phase for the sc(100) surface. In the case of the sc(110) surface a stronger modification is necessary. These trends are plausible: Obviously, for both surfaces a larger t_{11} means that electrons in the top layer are more itinerant, and thus tend to delay the transition to the insulating state as U is increased. A smaller intralayer coordination number q counteracts this mechanism. Consequently, one needs a stronger enhancement of t_{11} for the (110) surface. The U range where a metallic surface coexists with an insulating bulk quickly increases as t_{11} is increased. For $t_{11} \rightarrow \infty$ one would expect that the energy scales relevant for the bulk become meaningless, and that the electronic structure of the top layer decouples from the rest system. This is predicted correctly by Eq. (28) which yields $U_{c,\text{surf}} = 6t_{11}\sqrt{q}$ in this limit, i.e., the critical interaction strength of a free-standing two-dimensional layer.

B. Modified interlayer surface hopping

For a modified interlayer hopping between the top layer and the subsurface layer $t_{12} \neq t$, we have

$$a' = a, \quad b' = \frac{t_{12}^2}{t^2} b. \quad (29)$$

A metallic surface of a Mott insulating bulk is possible for

FIG. 2. t_{12} - U phase diagram.

$$t_{12} > 4\sqrt{2}t, \quad (30)$$

irrespective of the type of the surface. The critical interaction strength for the surface transition is given by

$$U_{c,\text{surf}} = 6t \sqrt{q+p} \frac{t_{12}^4}{t^2} \frac{1}{\sqrt{t_{12}^4 - t^4}}. \quad (31)$$

Figure 2 shows $U_{c,\text{surf}}$ as a function of t_{12} for the different surfaces.

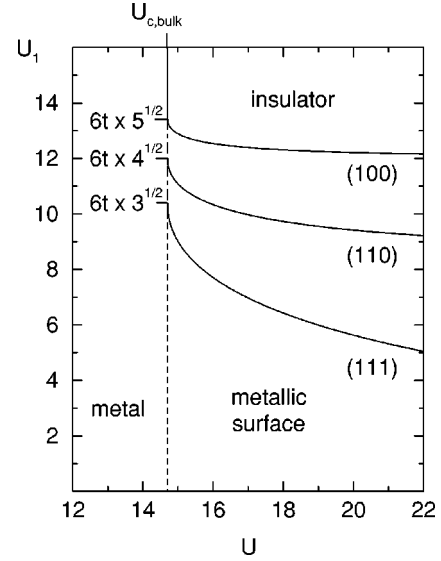
An enhancement of t_{12} again means an enhancement of the itinerancy of electrons at the surface. Hopping processes between the topmost and subsurface layers become more likely. A modification of about 19% is sufficient to suppress the transition to the Mott insulating phase at the surface for $U > U_{c,\text{bulk}}$. The surface critical interaction strength $U_{c,\text{surf}}$, up to which the metallic surface phase persists for a given t_{12} , is the largest for the sc(111) surface, since here the perpendicular hopping is favored by the comparatively high interlayer coordination number $p=3$. In the limit $t_{12} \rightarrow \infty$ the first two layers of the surface will decouple from the bulk. The surface critical interaction strength in this limit should be the same as for a bilayer system with strongly anisotropic hopping. Consider, for simplicity, the sc(111) surface where $q=0$. In this case all sites in the bilayer system have the same coordination number p and the bulk formula (20) may be applied accordingly. This yields $U_{c,\text{surf}} = 6t_{12}\sqrt{p}$, which is consistent with the $t_{12} \rightarrow \infty$ limit of Eq. (31).

C. Modified surface Coulomb interaction

Finally, we consider a modified Coulomb interaction in the top layer, $U_1 \neq U$. In this case,

$$a' = \frac{U^2}{U_1^2} a, \quad b' = \frac{U}{U_1} b. \quad (32)$$

As in the two other cases, we could fix the surface model parameters, vary U , and ask for the critical interaction strength $U_{c,\text{surf}}$. For the present case, however, it appears to be more intuitive to consider the bulk U to be a fixed quantity and to vary U_1 .

FIG. 3. U - U_1 phase diagram.

For U above the bulk critical interaction $U_{c,\text{bulk}}$ the bulk is a Mott insulator. The system may then become critical with respect to U_1 , provided that

$$U_1 < \sqrt{\frac{q+p}{q+2p}} U_{c,\text{bulk}}. \quad (33)$$

The surface transition takes place at $U_1 = U_{1,c,\text{surf}}$ with

$$U_{1,c,\text{surf}} = \sqrt{\frac{U^2 + 36qt^2}{2}} - \sqrt{\left(\frac{U^2 - 36qt^2}{2}\right)^2 - 36^2 p^2 t^4} \quad (34)$$

for $U > U_{c,\text{bulk}}$. Figure 3 shows the corresponding phase diagram. For $U \rightarrow \infty$ we obtain $U_{1,c,\text{surf}} = 6t\sqrt{q}$. This is the critical interaction strength of the free-standing monolayer.

The results for modified surface Coulomb interaction can be compared with Hasegawa's slave-boson approach.³⁰ Qualitatively, the respective U - U_1 phase diagrams for the sc(100) surface look similar. The critical interactions predicted by the slave-boson method are somewhat larger compared with the DMFT results. This is typical for the slave-boson method.⁵ An important difference is found with respect to the ‘‘special transition’’ at the tricritical point $U = U_{c,\text{bulk}}$, $U_1 = U_{1,c} \equiv \sqrt{(q+p)/(q+2p)} U_{c,\text{bulk}}$. The linearized DMFT predicts

$$\frac{U_{1,c,\text{surf}} - U_{c,\text{bulk}}}{U_{c,\text{bulk}}} \propto \left(\frac{U_1}{U_{1,c}} - 1 \right)^{1/\phi} \quad (35)$$

for $U_1 \rightarrow U_{1,c}$ with a ‘‘crossover exponent’’ $\phi=1/2$. The same crossover exponent is found for modified surface hopping t_{11} or t_{12} ,

$$\frac{U_{c,\text{surf}} - U_{c,\text{bulk}}}{U_{c,\text{bulk}}} \propto \left(\frac{t_{11(2)}}{t_{11(2),c}} - 1 \right)^{1/\phi}, \quad (36)$$

where $t_{11,c}$ and $t_{12,c}$ are defined by the right-hand sides of Eqs. (27) and (30), respectively. This follows from a direct calculation and can also be seen in Figs. 1, 2, and 3. Con-

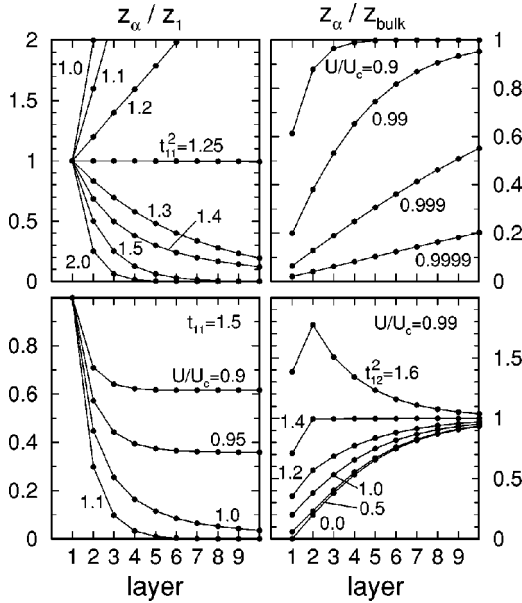


FIG. 4. Profiles of the quasiparticle weight for the sc(100) surface. Upper left: profiles for different t_{11} . $U = U_{c,\text{bulk}}$ for $t_{11} \leq 1.25$ and $U = U_{c,\text{surf}}$ for $t_{11} \geq 1.25$. Upper right: $t_{11} = t = 1$ and different U close to $U_{c,\text{bulk}}$. Lower left: $t_{11} = 1.5$ and different $U/U_{c,\text{bulk}}$. Lower right: $U/U_{c,\text{bulk}} = 0.99$ and different t_{12}^2 . The profiles are normalized to the top-layer value (right-hand side) or the bulk value (left-hand side), respectively.

versely, within the slave-boson theory of Ref. 30, $U_{1c,\text{surf}}$ seems to be constant as a function of U , and a crossover exponent cannot be defined.

D. Profiles of the quasiparticle weight

The mean-field equation of the linearized DMFT, $\Delta_{N+1}^{(\alpha)} = \sum_{\beta} K_{\alpha\beta} \Delta_N^{(\beta)}$, has a nontrivial solution only at a critical point for the Mott transition, e.g., at $U = U_{c,\text{bulk}}$ or $U = U_{c,\text{surf}}$. This solution is a fixed point of the matrix \mathbf{K} , $\Delta_{\infty}^{(\alpha)} = \lim_{N \rightarrow \infty} \Delta_N^{(\alpha)}$, and can be calculated as the eigenvector of \mathbf{K} belonging to the eigenvalue $\lambda = 1$ [Eq. (16)]. Since $z_{\alpha} \propto \Delta^{(\alpha)}$, the eigenvector has the meaning of the critical profile of the quasiparticle weight, i.e., the α dependence of z_{α} in the limit $z_{\alpha} \rightarrow 0$. It is uniquely determined up to a normalization constant.

The upper left part of Fig. 4 shows the critical profile at the sc(100) surface for different values of t_{11} and $U = U_{c,\text{bulk}}$ or $U = U_{c,\text{surf}}$, respectively. z_{α} has been normalized to its top-layer value z_1 . For unmodified surface hopping $t_{11} = t$, the profile is linear. In fact, the ansatz $z_{\alpha} \propto \alpha$ solves the mean-field equation $z_{\alpha} = (36t^2/U^2)(qz_{\alpha} + pz_{\alpha+1} + pz_{\alpha-1})$ for $U = U_{c,\text{bulk}} = 6t\sqrt{q+2p}$. Physically, this means that at the critical interaction the surface effects extend into the bulk up to *arbitrarily* large distances. Note that this implies that actually an infinite number of inequivalent surface layers has to be considered in a fully numerical evaluation of the DMFT.

For U close to $U_{c,\text{bulk}}$ but $U < U_{c,\text{bulk}}$, one would expect that the profile converges to a finite bulk value: $\lim_{\alpha \rightarrow \infty} z_{\alpha} = z_{\text{bulk}} > 0$. In its present form, however, the linearized DMFT is not applicable here. One may consider the follow-

ing extension²² of the mean-field equation (for simplicity, we discuss the case of uniform model parameters, the generalization for modified surface hopping or $U_1 \neq U$ is straightforward):

$$z_{\alpha} = \frac{36t^2}{U^2}(qz_{\alpha} + pz_{\alpha+1} + pz_{\alpha-1}) - cz_{\alpha}^2. \quad (37)$$

A quadratic term in z_{α} with a constant coefficient $c > 0$ has been added. The constant c can be fixed by the value for z_{bulk} or for z_1 (Ref. 22 yields the explicit value $c = 11/9$, but we do not need the result here). This extension of the linearized DMFT is in the spirit of Landau theory, we simply consider the next term in an expansion with respect to the ‘‘order parameter’’ z_{α} . As in the Landau theory, higher-order terms in z_{α} or quadratic terms that couple the different layers are still neglected. The additional term in Eq. (37) ensures a linear U dependence of the quasiparticle weight in each layer: $z_{\alpha} \propto (U_c - U)$ for $U \rightarrow U_c$. This is consistent with the (bulk) critical behavior found within the PSCM.²¹

Using Eq. (37) we have calculated the profile of the quasiparticle weight for $t_{11} = 1$ and different $U < U_{c,\text{bulk}}$; see Fig. 4 (upper right). For $U/U_{c,\text{bulk}} = 0.9$ the quasiparticle weight differs significantly from the bulk value in the first few layers from the surface only. As $U \rightarrow U_{c,\text{bulk}}$, however, the linear trend of z_{α} clearly develops.

A linear trend of the critical profile is also observed for slightly enhanced surface hopping, $t_{11}^2 = 1.1$ and $t_{11}^2 = 1.2$ (Fig. 4, upper left). For a surface hopping $t_{11} = \sqrt{1+p/q} = \sqrt{5}/4$ we obtain the so-called special transition [cf. Eq. (27) and Fig. 1]. At the critical interaction the profile is a constant (Fig. 4, upper left). In this case the effect of missing neighbors at the surface is exactly compensated for by the enhancement of t_{11} .

For $t_{11} > \sqrt{5}/4$ there are two critical interactions, $U_{c,\text{bulk}}$ and $U_{c,\text{surf}}$. For $U = U_{c,\text{surf}}$, z_{α}/z_1 is at its maximum in the top layer and exponentially decays as $\alpha \rightarrow \infty$ (Fig. 4, upper left). For $U < U_{c,\text{surf}}$ [according to Eq. (37)] the decay becomes slower until the profile converges to a finite bulk value for $U < U_{c,\text{bulk}}$ (lower left).

Finally, the lower right part of Fig. 4 shows the profile of the quasiparticle weight obtained from Eq. (37) for $U/U_{c,\text{bulk}} = 0.99$ and modified interlayer surface hopping t_{12} . For $t_{12}^2 < \sqrt{2}$ the profile is a monotonously increasing function when passing from the surface to the bulk. $t_{12}^2 = \sqrt{2}$ marks the special transition [see Eq. (30)]. Here the profile would be constant for $\alpha \geq 2$ and $U = U_{c,\text{bulk}}$ as can be seen from the mean-field equation of the linearized DMFT. For $t_{12}^2 > \sqrt{2}$ the quasiparticle weight is enhanced at the surface, and decreases monotonously for $\alpha \geq 2$.

E. Infinite dimensions

Dynamical mean-field theory rests on the local approximation for the self-energy functional. Since it is known that in the limit of high spatial dimensions $D \rightarrow \infty$,³ the local approximation becomes exact,⁴⁴ it may be interesting to discuss the (somewhat artificial) case of a surface of the infinite-dimensional hypercubic lattice.

A D -dimensional hypercubic lattice may be thought to be built up from $(D-1)$ -dimensional ‘‘layers’’ perpendicular

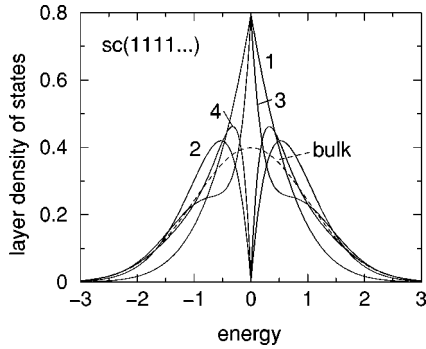


FIG. 5. $U=0$ layer-dependent density of states $\rho_\alpha^{(0)}(E)$ at the (1111...) surface of the $D=\infty$ hypercubic lattice. Scaled hopping $t=t^*/\sqrt{2D}$ with $t^*=1$. ‘‘1’’ stands for the topmost surface layer, ‘‘2’’ denotes the subsurface layer, etc.

to a D -dimensional spatial direction characterized by the set of Miller indices $[x_1, x_2, \dots, x_D]$. Cutting the hopping between two adjacent layers, one obtains a ‘‘ (x_1, x_2, \dots, x_D) surface.’’ Consider the low-index directions with $x_1 = \dots = x_r = 1$ and $x_{r+1} = \dots = x_D = 0$. For a given site there are $q=2D-2r$ nearest neighbors within the same layer and $p=r$ nearest neighbors in each of the adjacent layers ($Z=q+2p=2D$).

For $r=1$, i.e., a (1000...) surface, a site in the topmost layer has $Z_S=q+p=2D-1$ nearest neighbors, to be compared with $Z=2D$ in the bulk. For $D \rightarrow \infty$ the local environment of the surface sites is essentially the same as in the bulk, surface effects become meaningless. With the usual scaling of the hopping $t=t^*/\sqrt{2D}$,³ the free top-layer local density of states (DOS) is a Gaussian $\rho^{(0)}(E) = \exp[-(E/t^*)^2/2]/(\sqrt{2\pi}t^*)$ —as in the bulk.

For $r=D$ one obtains the open (1111...) surface. The surface coordination number is reduced to $Z_S=p=D$. This implies a ratio $\Delta_S/\Delta = Z_S/Z = (q+p)/(q+2p) = 0.5$ between the variances of the top-layer and bulk DOS. The results of a simple numerical calculation are shown in Fig. 5. We notice a strongly modified and strongly layer-dependent DOS near the surface which slowly converges to the bulk Gaussian DOS for $\alpha \rightarrow \infty$. In many respects the results resemble the DOS at the $D=3$ sc(111) surface, in particular the oscillation of $\rho_\alpha^{(0)}(E=0)$ as a function of α .⁴⁵

In infinite dimensions dynamical mean-field theory is exact also for the semi-infinite model. The scaling of the hopping implies $G_{ij}^{(0)} \sim 1/\sqrt{D}$ for the free propagator between arbitrary nearest-neighbor sites i and j , and the proof that the self-energy is local, is essentially unchanged (see Refs. 3, 4, and 44). The simple linearized DMFT can be developed as in Sec. IV. We only have to insert the general expressions for the coordination numbers $q=2D-2r$ and $p=D$, and to perform the limit $D \rightarrow \infty$ in the Eqs. (27)–(34), paying attention to the scaling of the hopping.

Varying r we can then pass continuously from the most closed ($r=1$) to the most open ($r=D$) surface geometry. Consider, for example, a modified intralayer surface hopping. A surface phase is predicted to be existing for $t_{11}^* > t^* \sqrt{1+r/(2D-2r)}$ [cf. Eq. (27)]; i.e., for all $t_{11}^* > t^*$ in the case of the closed $r=1$ surface and not at all for the $r=D$ surface. For $r=1$ the surface critical interaction is given by $U_{c,\text{surf}} = 6t_{11}^*$ [Eq. (28)] to be compared with the bulk

critical interaction $U_{c,\text{bulk}} = 6t^*$ [Eq. (20)]. With increasing r , $U_{c,\text{surf}}$ decreases until $U_{c,\text{surf}} = U_{c,\text{bulk}}$ for $r=D$.

The other cases may be discussed accordingly. Upon taking the limit $D \rightarrow \infty$, we always obtain nontrivial and plausible results. The discussion is analogous to the $D=3$ case. We conclude that the semi-infinite Hubbard model remains nontrivial for $D=\infty$ and provides a useful framework for investigating the surface phase. In principle, this can be done without approximations by employing the DMFT. Recall, however, that the linearized DMFT is still approximate (Sec. IV and Ref. 22).

VI. EXACT-DIAGONALIZATION METHOD

For a complete numerical solution of the mean-field equations at finite temperatures one may employ the quantum Monte Carlo method.^{37,46,47} For $T=0$ the ED approach^{28,41,42} can be applied and is chosen here. The main idea is to map onto a SIAM with a finite number of sites n_s . The Lanczs technique⁴⁸ is used to calculate the ground state as well as the $T=0$ impurity Green function and self-energy. The DMFT equations are solved on the discrete mesh of Matsubara energies where the (fictitious) inverse temperature $\tilde{\beta}$ introduces a low-energy cutoff. Details of the method can be found in Ref. 5. The surface geometry can be simulated by a slab consisting of a finite but sufficiently large number of layers d (for $U \neq U_c$). The numerical effort then increases linearly with d at least. In Refs. 23 and 29 we have discussed the application of ED to film and surface geometries.

ED is able to yield the essentially exact solution of the mean-field equations in a parameter range where the errors introduced by the finite system size are unimportant. For the Mott problem the relevant low-energy scale is set by the width of the quasiparticle peak in the metallic solution. It has to be expected that there are non-negligible finite-size effects when this energy scale becomes comparatively small. We are thus limited to interaction strengths that are not too close to $U_{c,\text{bulk}}$ or $U_{c,\text{surf}}$, and cannot access the very critical regimes. This also implies that a precise determination of $U_{c,\text{bulk}}$ and $U_{c,\text{surf}}$ and thereby a direct comparison with the linearized DMFT is not possible. The discussion in Ref. 23, however, shows that the main trends can be derived safely.

In the following we mainly focus on the low-energy electronic structure which the ED method is able to predict reliably in the noncritical regimes. The so-called layer-dependent quasiparticle weight,

$$z_\alpha = \left(1 - \frac{d\Sigma_\alpha(E=0)}{dE} \right)^{-1}, \quad (38)$$

is the primary quantity of interest. $z_\alpha \leq 1$ is weight of the coherent quasiparticle peak in the local DOS $\rho_\alpha(E)$ of the α th layer or, alternatively, the reduction factor of the discontinuous drops in α th momentum-distribution function $n_{\alpha,\mathbf{k}}$ when \mathbf{k} crosses the one-dimensional Fermi ‘‘surfaces.’’²³

Routinely, the calculations have been performed with $n_s = 8$ sites in the effective impurity problems. For the fictitious temperature we have chosen $\tilde{\beta}^{-1} = 0.0016W$ ($W=12$ is the free bandwidth). n_s and $\tilde{\beta}$ determine the ‘‘energy resolution’’ which is found to be about $\Delta E = 0.12 = W/100$. This implies that reliable results can be expected in a parameter

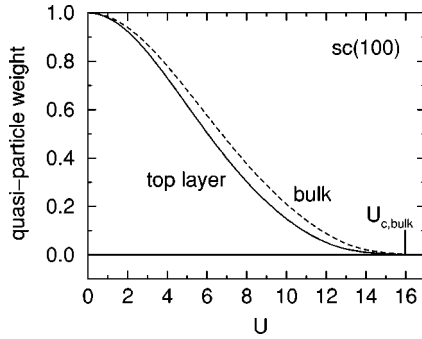


FIG. 6. U dependence of the quasiparticle weight in the bulk and in the top layer for the sc(100) surface (uniform model parameters) as obtained from the ED method for $n_s=8$. $U_{c,\text{bulk}} \approx 16.0$. $t=1$ sets the energy scale.

region where $z_\alpha > 0.01$ (cf. Ref. 29). A moderate number $d \leq 25$ of layers in the slab is sufficient to simulate the semi-infinite system—except for the very critical regime. This has been checked by comparing the results from calculations for different d . We made use of the mirror symmetry at the center of the slab and of electron-hole symmetry to reduce the number of parameters, the conduction-band energies ϵ_k , and the hybridization strengths V_k ($k=2, \dots, n_s$), which have to be determined self-consistently. We always found a unique and fully stabilized solution.

VII. NUMERICAL RESULTS FOR THE sc(100) SURFACE

To keep the calculations manageable, we restrict the discussion to the $D=3$ sc(100) surface in the following. We start with the case of uniform model parameters. Figure 6 shows the bulk quasiparticle weight z (dashed line) as a function of U . It starts from its noninteracting value $z=1$. A quadratic U dependence is noticed for small U in agreement with perturbation theory.²⁹ z vanishes as U approaches $U_{c,\text{bulk}}$. The overall dependence on U is very similar to what is known from DMFT studies of the $D=\infty$ Bethe lattice.⁵

In the top layer of the sc(100) surface the quasiparticle weight is significantly reduced (solid line). The lowered coordination number at the surface implies a reduced variance Δ_S of the free surface DOS, and thereby an increased effective interaction $U/\sqrt{\Delta_S}$ compared with the bulk. Thus at the surface correlation effects are enhanced, and $z_{\alpha=1}$ is lowered. Despite this *tendency* toward an insulating surface, we find a common critical interaction $U_{c,\text{surf}}=U_{c,\text{bulk}}$ which, for uniform parameters, is in agreement with the analytical results. $U_{c,\text{bulk}}$ also represents the critical interaction for all subsurface layers. For the rather closed (100) surface, $z_\alpha(U)$ is almost identical with the bulk function for $\alpha \geq 2$.

From Fig. 6 we can read off $U_{c,\text{bulk}} \approx 16.0$, while Eq. (20) predicts $U_{c,\text{bulk}}=14.7$. We have to bear in mind, however, the underlying assumptions that lead to Eq. (20). Moreover, as concerns the ED, finite-size effects prevent a precise estimate: $U_{c,\text{bulk}} \approx 15.1$ is found for $n_s=10$ sites in the impurity models.²⁹ On the other hand, comparing the results for $n_s=8$ and $n_s=10$, there are no significant changes as long as $z_\alpha > 0.01$.²⁹ This means (see Fig. 6) that the overall layer and U dependence is predicted reliably. We also believe that the finding of a common critical interaction is not an artifact of

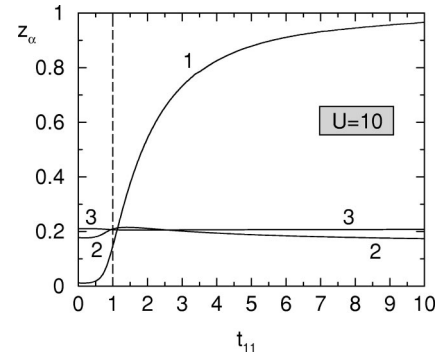


FIG. 7. Quasiparticle weight of the top layer ($\alpha=1$) and the subsurface layers ($\alpha=2$ and 3) for $U=10 < U_{c,\text{bulk}}$ as a function of the modified intralayer surface hopping t_{11} . $t=1$.

the ED approach since this is made plausible by the linearized DMFT.

At the critical interaction the metallic solution continuously coalesces with the insulating solution that is found for $U > U_{c,\text{bulk}}$. The insulating solution persists down to another (common) critical interaction strength $U_{c,1} < U_{c,\text{bulk}}$ (we find $U_{c,1} \approx 11.5$). In the coexistence region, however, it is thermodynamically irrelevant. For details, we refer to Refs. 5, 42, 19, and 23.

A. Modified intralayer surface hopping

A modification of the model parameters at the very surface may strongly affect the quasiparticle weight. As in Sec. V we first consider a modified hopping within the top layer: $t_{11} \neq t$.

Figure 7 gives an overview for fixed Coulomb interaction $U=10$. The above-mentioned tendency toward an insulating surface is enhanced when t_{11} is decreased. The top-layer quasiparticle weight quickly decreases, but even for $t_{11}=0$ it does not vanish completely. For $t_{11} > t$ one can see the opposite trend. $z_{\alpha=1}$ increases with increasing t_{11} . In the limit $t_{11} \rightarrow \infty$ it approaches its noninteracting value $z_{\alpha=1}=1$. For $t_{11}=10t$ the low-energy electronic structure is almost perfectly decoupled. In the top surface layer there is a quasiuncorrelated motion of the electrons ($z_{\alpha=1}=0.98$ at $U/t_{11}=1$). The rest system, however, remains a strongly correlated Fermi liquid.

For the subsurface layers, the dependence of the quasiparticle weight on t_{11} is comparatively weak. Figure 8 shows z_α for $\alpha \geq 2$. On the enlarged scale in Fig. 8 there is still a

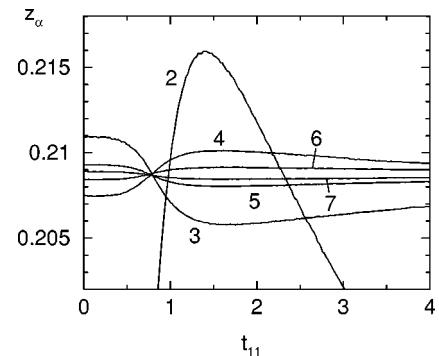


FIG. 8. The same as Fig. 7 but on an enlarged scale.

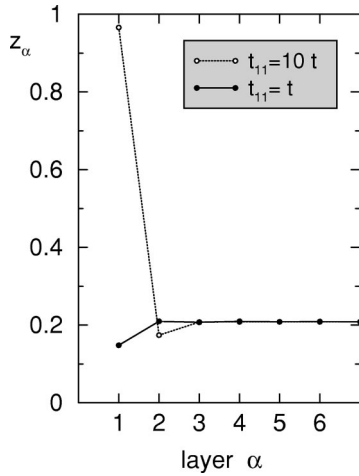


FIG. 9. Layer dependence of the quasiparticle weight for uniform model parameters as well as strongly enhanced intralayer surface hopping. $U=10$.

considerable t_{11} dependence of $z_{\alpha=2}$ (second layer). For $\alpha \rightarrow \infty$, however, i.e., with increasing distance to the surface, this dependence diminishes: The bulk quasiparticle weight obviously cannot be affected by the surface modification of the hopping parameter. We also notice that there is a nearly constant quasiparticle weight for $t_{11} \approx 0.8t$ and all $\alpha \geq 3$.

For fixed t_{11} one finds an oscillating layer dependence of z_{α} . This is demonstrated in Figs. 9 and 10 for $t_{11}=t$ and $t_{11}=10t$. For the strongly perturbed system with $t_{11}=10$, the layer dependence is somehow irregular in the near-surface region, oscillations do not build up until $\alpha \geq 5$. In both cases the oscillation is strongly damped. For $\alpha=13$ we have $\Delta z/z \approx 2 \times 10^{-4}$. Thus, for a film with thickness $d=25$, the quasiparticle weight is nearly constant at the film center. Furthermore, the differences between the uniform and perturbed systems become smaller and smaller with increasing distance to the surface. The observed oscillations can be traced back to oscillations of the free layer DOS at the Fermi energy. It is well known⁴⁹ that the presence of the surface gives rise to a layer-by-layer oscillation of $\rho_{\alpha}(E=0)$ for $U=0$. For the present case (local self-energy, manifest particle-hole symmetry, metallic phase), the density of states at the Fermi edge is unrenormalized by the interaction [see Eq. (10) and Ref. 23]. The same oscillation is thus found for $\rho_{\alpha}(E=0)$ at any $U < U_{c,\text{bulk}}$, and will also lead to oscillations of the low-energy part of the Green function and thereby to oscillations

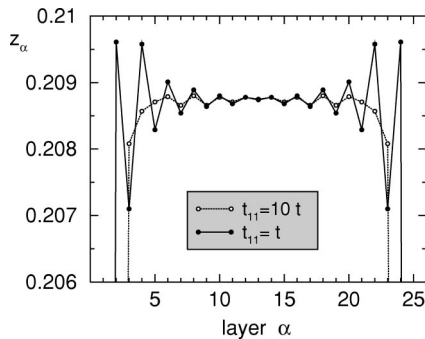


FIG. 10. The same as Fig. 9 but on an enlarged scale. Slab thickness: $d=25$.

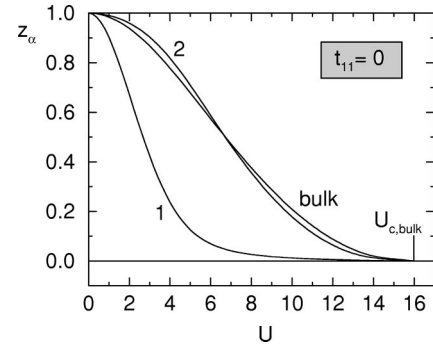


FIG. 11. U dependence of z_{α} when the intralayer surface hopping is switched off.

of the low-energy part of the self-energy. Finally, the oscillating behavior of z_{α} for $U=10$ shows that we are well below the critical point: For U close to $U_{c,\text{bulk}}$ we expect a monotonous behavior from the linearized DMFT (see Fig. 4).

Let us now tackle the question of surface phases. The scenario of an insulating surface coexisting with a metallic bulk was excluded by the linearized DMFT. The same is found by the numerical evaluation of the DMFT: Fig. 11 shows the layer-dependent quasiparticle weight for $t_{11}=0$, where the strongest suppression of $z_{\alpha=1}$ is expected. In fact, the top-layer quasiparticle weight quickly decreases as a function of U and, compared with the bulk value, becomes very small above $U \approx 6$. However, we find a nonzero weight in the top layer up to $U=U_{c,\text{bulk}}$, which implies $U_{c,\text{surf}} = U_{c,\text{bulk}}$. Between $U \approx 6$ and $U=U_{c,\text{bulk}}$ we may speak of an *induced* metallic surface according to the discussion in Sec. V.

The linearized DMFT predicted a metallic surface on top of a Mott-insulating bulk to be possible for $t_{11} > t\sqrt{5/4}$. We choose $t_{11}=1.5t$ for the numerical calculation to be well above this threshold. Figure 12 proves that two different critical interactions are found. Over the whole U range considered, the top-layer quasiparticle weight is strongly enhanced compared with the bulk and is finite also at $U=U_{c,\text{bulk}}$ where the bulk weight vanishes. Note that $z_{\alpha=1}(U)$ is continuous at $U=U_{c,\text{bulk}}$. The top-layer quasiparticle weight approaches zero at $U=U_{c,\text{surf}}=20.0$, which marks the surface transition point while the extraordinary transition takes place at $U=U_{c,\text{bulk}}=16.0$.

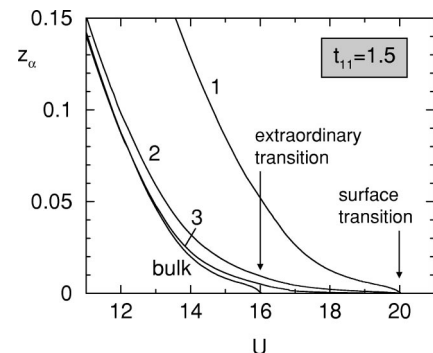


FIG. 12. U dependence of z_{α} for enhanced intralayer surface hopping. Surface transition at $U=U_{c,\text{surf}}$. Extraordinary transition at $U=U_{c,\text{bulk}}$.

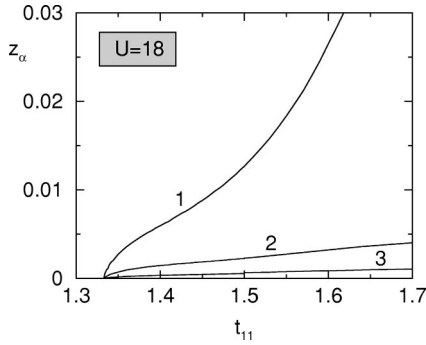


FIG. 13. z_α as a function of t_{11} for $U > U_{c,\text{bulk}}$.

Evaluating the analytical formula for the surface critical interaction [Eq. (28)] for the present case, we obtain $U_{c,\text{surf}} = 18.2$, which agrees well with the numerical result if one takes into account that for the bulk critical interaction the linearized theory also yields a somewhat smaller value. We also expect that $U_{c,\text{surf}}$ (as $U_{c,\text{bulk}}$) is overestimated by the ED due to finite-size effects.^{23,29} While finite-size effects prevent a precise determination of the critical interactions, they are irrelevant concerning the very existence of the metallic surface phase. Even for U well above $U_{c,\text{bulk}}$, the top-layer quasiparticle weight is still larger than $z_{\alpha=1} = 0.01$, and thus the ED for $n_s = 8$ is still able to resolve the energy scale set by the width of the Kondo-type resonance at the surface.

Since the low-energy surface excitations cannot propagate into the bulk for $U > U_{c,\text{bulk}}$ but are reflected at the bulk Hubbard gap, the Kondo resonance represents a true surface state. Therefore, its amplitude must decay exponentially with increasing distance to the surface. Figure 12 shows that some weight is induced in the subsurface layers which rapidly decreases.

The surface transition is also found as a function of t_{11} for fixed interaction $U > U_{c,\text{bulk}}$. Figure 13 shows the numerical results for $U = 18$. When $t_{11} > t_{11,c} = 1.33t$, the surface becomes metallic. The critical value may be compared with $t_{11,c} = 1.48t$ which is obtained by solving Eqs. (16) and (23) for t_{11} .

For the t_{11} range considered in Fig. 13, the number of layers in the slab d that is necessary to simulate the actual surface can be lowered down to $d \approx 5$: We performed calculations for different thicknesses d ; there are hardly any differences between the results for z_α at the surface as long as $d \geq 5$. This is interpreted as follows: Since the coherent part of the bulk spectrum has disappeared for $U > U_{c,\text{bulk}}$, the surface electronic structure is essentially decoupled from the bulk in the low-energy regime. The decoupling at the low-energy scale is indicated by the rapid decrease of z_α with increasing α (see Fig. 13). Conversely, on the high-energy scale set by the charge excitations, bulk and surface modes cannot decouple. There is always a finite energetic overlap of the bulk and the surface DOS since t_{11} mainly changes the effective widths but not the positions of the Hubbard peaks in the surface DOS. The effect of the Hubbard bands on the low-energy features, however, seems to be rather weak since otherwise a change of d would lead to significant changes in the surface low-energy electronic structure by indirect coupling between low- and high-energy surface excitations and high-energy surface and bulk excitations. The surface Kondo

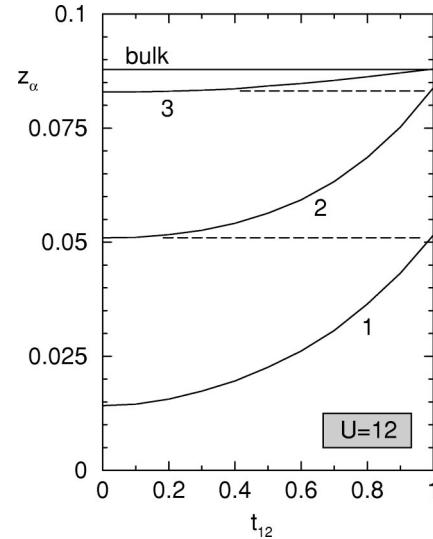


FIG. 14. Layer-dependent quasiparticle weight for $U < U_{c,\text{bulk}}$ as a function of the interlayer surface hopping $t_{12} \leq t = 1$.

resonance in the metallic surface phase is spatially confined to the first few layers, and energetically isolated from the surface Hubbard bands.

B. Modified interlayer surface hopping

A complete decoupling between the top layer and the rest system is obtained for vanishing interlayer surface hopping $t_{12} = 0$. Figure 14 shows the layer-dependent quasiparticle weight as a function of t_{12} . While for $U = 10$ we noticed an oscillating layer dependence for uniform hopping (Figs. 9 and 10), there is a monotonous layer dependence for $U = 12$ (Fig. 14, for $t_{12} = 1$). This is the typical behavior when the system is close to criticality as has been noted before (cf. Ref. 29, and the discussion of the analytical z_α profiles in Sec. V). The layer dependence remains monotonous for $t_{12} \rightarrow 0$. For $t_{12} = 0$ we have essentially two independent systems. The isolated top layer is still metallic. In the rest system the $\alpha = 2$ layer represents the new top layer, the $\alpha = 3$ layer becomes the first subsurface layer, and so on. This implies that the value of z_α for $t_{12} = 0$ must be equal to the value of $z_{\alpha-1}$ for $t_{12} = 1$. These relations are indicated by the dashed lines in Fig. 14. They represent a nontrivial check of the numerics.

An effective separation into subsystems is also observed in the opposite limit of a strongly enhanced interlayer surface hopping. Figure 15 shows that $z_{\alpha=1}$ and $z_{\alpha=2}$ approach their noninteracting values, while for $\alpha \geq 3$ the quasiparticle weight changes only slightly as $t_{12} \rightarrow \infty$. In the low-energy regime the electronic structure of the first two layers decouples from the rest system. The value of z_α for all $\alpha \geq 3$ approaches the value of $z_{\alpha-2}$ for $t_{12} = 1$ (see the inset).

A somewhat artificial realization of an insulating surface phase on top of a metallic bulk can be obtained for $t_{12} \rightarrow 0$ by choosing $U_{c,D=2} < U < U_{c,\text{bulk}}$, where $U_{c,D=2}$ is the critical interaction of the two-dimensional layer. For $U > U_{c,D=2}$ the top layer must become insulating when it is decoupled from the rest system ($t_{12} = 0$). This is demonstrated in Fig. 16. The figure also shows that the top layer becomes metallic (with a very small quasiparticle weight) as soon as an arbitrarily small interlayer hopping is switched on.

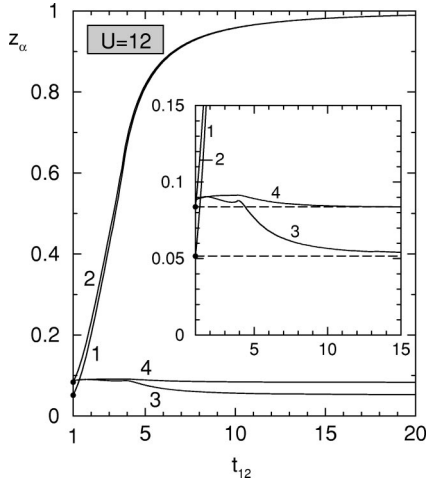


FIG. 15. The same as Fig. 14 but for $t_{12} \geq t = 1$. Inset: asymptotic behavior of z_α .

Finally, Fig. 17 shows the extraordinary and the surface transition for fixed $t_{12} = 3.0$. The surface critical interaction can be read off to be $U_{c,\text{surf}} = 23.8$, while the linearized DMFT with $U_{c,\text{surf}} = 21.7$ [Eq. (31)] again predicts a slightly smaller critical value.

C. Modified surface Coulomb interaction

We finally discuss the modification of the surface Coulomb interaction U_1 . Figure 18 shows the quasiparticle weight z_α for $\alpha = 1, 2$, and 3 and z_{bulk} as a function of U_1/U , where U is fixed at $U = 10$. On decreasing U_1 ($U_1 < U$), z_1 quickly increases, and for $U_1 \rightarrow 0$ it approaches the noninteracting value $z_1 = 1$.

For enhanced $U_1 > U$ the top-layer quasiparticle weight is decreased but remains finite even for large values of U_1 , i.e., we again find an *induced* metallic surface. Asymptotically, however, the top-layer weight approaches zero: $z_1 \rightarrow 0$ for $U_1 \rightarrow \infty$. In this limit the low-energy resonance in the top-layer DOS essentially disappears and a large Hubbard gap $\sim U_1$ opens. This implies that—in the low-energy regime—the subsurface ($\alpha = 2$) DOS for $U_1 \rightarrow \infty$ must become iden-

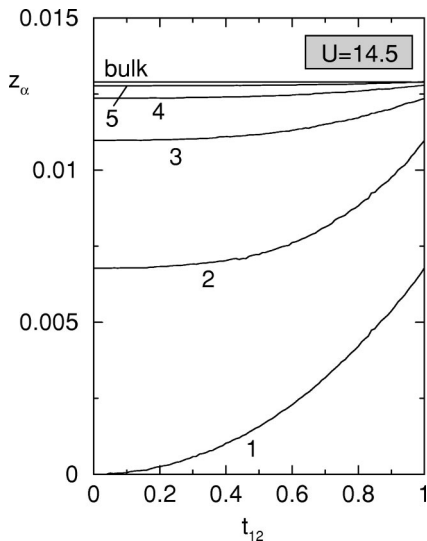


FIG. 16. The same as Fig. 14 but for $U_{c,D=2} < U < U_{c,\text{bulk}}$.

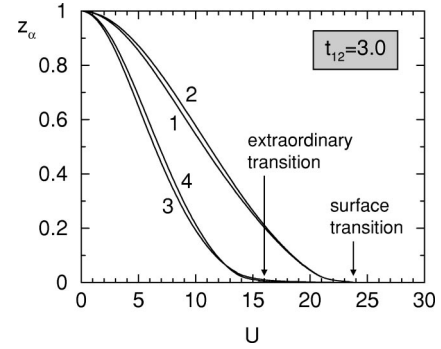


FIG. 17. U dependence of z_α for enhanced interlayer surface hopping t_{12} .

tical with the $U_1 = U$ surface ($\alpha = 1$) DOS. For $U_1 \rightarrow \infty$ we thus expect $z_2(U_1 \rightarrow \infty) = z_1(U_1 = U)$, and consequently $z_\alpha(U_1 \rightarrow \infty) = z_{\alpha-1}(U_1 = U)$ for all α . In fact, this “shift” of the surface by one layer can be seen in Fig. 18 and in the inset: For $U_1/U = 5$ only small differences still remain between z_α and $z_{\alpha-1}(U_1 = U)$.

The shift $\alpha \rightarrow \alpha - 1$ also implies that the oscillating layer dependence of z_α for $U_1 = U$ must be reversed for $U_1 \rightarrow \infty$: Minima are replaced by maxima, and vice versa. This partly explains that between (at $U_1/U \approx 1.2$) the quasiparticle weight is nearly layer independent.

According to the linearized DMFT, a metallic surface on top of an insulating bulk can be found if $U_1 < 6t\sqrt{5}$ [Eq. (33)] and $U > U_{c,\text{bulk}} = 6t\sqrt{6}$. If we fix the ratio $U_1/U = 0.5$ and vary U , the surface transition should occur at $U_{1,c,\text{surf}} = 12.1$ [set $U = 2U_{1,c,\text{surf}}$ in Eq. (34) and solve for $U_{1,c,\text{surf}}$]. The result of the numerical solution of the DMFT equations is shown in Fig. 19. Again, the numerically obtained value, $U_{1,c,\text{surf}} = 0.5 \times 26.3 = 13.15$, is somewhat larger than the analytical prediction—the discussion is the same as for the modified surface hopping.

At the extraordinary transition $U = U_{c,\text{bulk}}$, the quasiparticle weight in the top- (not shown in Fig. 19) and in the first

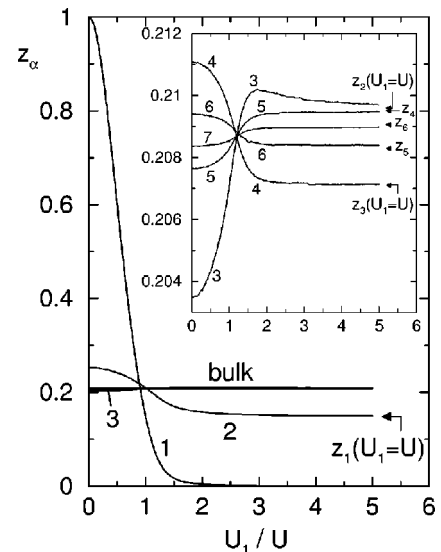


FIG. 18. Layer-dependent quasiparticle weight for $U = 10 < U_{c,\text{bulk}}$ and modified Coulomb interaction in the top layer U_1 . The arrow indicates the value of $z_{\alpha=1}$ for $U_1 = U$. In the inset, the arrows indicate the $U_1 = U$ values of z_α .

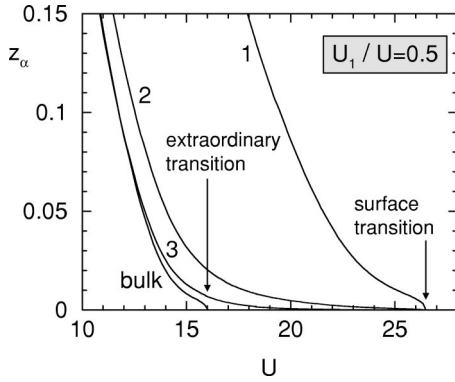


FIG. 19. U dependence of z_α for enhanced surface Coulomb interaction $U_1/U = \text{const}$.

subsurface layers are smooth functions of U . This is contrary to the results found within the slave-boson theory,³⁰ where the band-narrowing factor in the top layer shows up a discontinuous derivative at $U = U_{c,\text{bulk}}$. We believe, however, that this is an artifact due to incorrect boundary conditions. That is, only the first two surface layers are treated as “free” in the self-consistent calculation, while the $\alpha=3$ layer was already assumed to be bulklike in Ref. 30. As is known from the mean-field theory of localized spin models,⁵⁰ such boundary conditions may result in artificial singularities at the extraordinary transition.

VIII. CONCLUSION

We have investigated the (Mott) metal-insulator transition at surfaces within the framework of the semi-infinite Hubbard model at half-filling and $T=0$. Basically, two approximations have been used:

First, the self-energy functional has been assumed to be reasonably local. This approximation sets the basis for the dynamical mean-field theory: The semi-infinite Hubbard model is self-consistently mapped onto a set of indirectly coupled impurity models corresponding to the inequivalent layers parallel to the surface. With the usual scaling of the (intralayer and interlayer) hopping, the approach becomes exact in the limit of infinite spatial dimensions. It has been shown that there are nontrivial surface effects even for $D = \infty$. Mainly, however, the DMFT has been used as a (mean-field) approach to study the $D=3$ low-index surfaces of the simple-cubic lattice.

Second, for the approximate solution of the impurity models, we have used the exact diagonalization of finite systems. The ED method allows us to deal systematically with a large number of geometries and model parameters. However, the method cannot access the very critical regime for the Mott transition because of errors due to finite-size effects. Directly at the critical point, we have alternatively considered a simplification of the mean-field equations (linearized DMFT). This analytical approach is also approximate. However, a convincing qualitative and (as far as can be judged) also quantitative agreement with the numerical ED results has been found. Referring to the points mentioned in the introduction, our results can be summarized as follows.

(1) The metal-insulator transition in the bulk of the semi-infinite system occurs exactly at the same critical interaction

$U_{c,\text{bulk}}$ as for the infinitely extended system: $U_{c,\text{bulk}} = U_c$.

(2) There is a nontrivial layer dependence of the quasiparticle weight, even (asymptotically) at the critical point. The z_α profile strongly depends on the model parameters at the surface, e.g., the hopping within the top layer t_{11} , the hopping between the top layer and the subsurface layer t_{12} , and the top-layer Coulomb interaction U_1 . There is a qualitative change of the profile if certain critical values $t_{11,c}$, $t_{12,c}$, and $U_{1,c}$ are exceeded. These critical values are found to be of a realistic order of magnitude.

(3) For uniform model parameters the top-layer quasiparticle weight z_1 is smaller than the bulk value z_{bulk} , since a reduced surface coordination number implies correlation effects to be effectively stronger at the surface. For interactions well below U_c , there is always an oscillating layer dependence of the quasiparticle weight. With increasing distance to the surface ($\alpha \rightarrow \infty$), this oscillation is strongly damped. In the critical regime, on the contrary, z_α monotonously increases with increasing α , and finally, for $U = U_c$ the critical profile is linear: $z_\alpha \propto \alpha$. For uniform model parameters there is a finite weight in the top layer ($z_1 > 0$) for $U < U_c$ only, i.e., only when the bulk is metallic. The transition at U_c is termed the “ordinary transition.”

(4) For a sufficiently strong modification of the surface model parameters ($t_{11} > t_{11,c}$, $t_{12} > t_{12,c}$, $U_1 < U_{1,c}$), the surface becomes metallic below a critical interaction $U_{c,\text{surf}} > U_{c,\text{bulk}}$ (“surface transition”). For $U_{c,\text{bulk}} < U < U_{c,\text{surf}}$, the quasiparticle weight exponentially decays from its maximum value z_1 at the surface toward zero in the bulk. At $U = U_{c,\text{bulk}}$ the bulk undergoes the transition to the metallic state (“extraordinary transition”). The top-layer quasiparticle weight is a smooth function of U even at $U = U_{c,\text{bulk}}$.

(5) The transition at $U = U_{c,\text{surf}} = U_{c,\text{bulk}}$ is called the “special transition.” Here the critical profile of the quasiparticle weight is flat $z_\alpha = z_{\text{bulk}} = \text{const}$ (at least for $\alpha \geq 2$). In this situation the effect of missing neighbors at the surface is compensated for by the change of the surface model parameters.

(6) There are two critical exponents that are merely related to the critical interactions; the “shift exponent” λ_s and the “crossover exponent” ϕ . They describe the trend of the U_c for a film of finite thickness d in the limit $d \rightarrow \infty$ and the trend of the surface critical interaction for the semi-infinite system near the special transition, respectively. Within the linearized DMFT, one finds $\lambda_s = 2$ and $\phi = 1/2$.

(7) For any realistic choice of the model parameters, a metallic bulk induces a metallic surface with $z_1 > 0$. Thus a Mott-insulating surface of a correlated metal is impossible. There are essentially two more or less trivial exceptions: The first is the static decoupling of the top layer for $t_{12} = 0$ at an interaction strength that is smaller than $U_{c,\text{bulk}}$ but larger than the critical interaction of the two-dimensional system. The second is a dynamical decoupling which occurs for infinite surface interaction $U_1 \rightarrow \infty$. Here the top-layer quasiparticle weight vanishes asymptotically.

ACKNOWLEDGMENT

This work was supported by the Deutsche Forschungsgemeinschaft within the SFB 290.

- ¹N.F. Mott, Proc. R. Soc. London, Ser. A **62**, 416 (1949).
- ²N.F. Mott, *Metal-Insulator Transitions* (Taylor and Francis, London, 1990).
- ³W. Metzner and D. Vollhardt, Phys. Rev. Lett. **62**, 324 (1989).
- ⁴D. Vollhardt, in *Correlated Electron Systems*, edited by V.J. Emery (World Scientific, Singapore, 1993), p. 57.
- ⁵A. Georges, G. Kotliar, W. Krauth, and M.J. Rozenberg, Rev. Mod. Phys. **68**, 13 (1996).
- ⁶F. Gebhard, *The Mott Metal-Insulator Transition* (Springer, Berlin, 1997).
- ⁷F. Englert, Phys. Rev. **129**, 567 (1963).
- ⁸M.C. Gutzwiller, Phys. Rev. Lett. **10**, 159 (1963).
- ⁹J. Hubbard, Proc. R. Soc. London, Ser. A **276**, 238 (1963).
- ¹⁰J. Kanamori, Prog. Theor. Phys. **30**, 275 (1963).
- ¹¹A. Georges and G. Kotliar, Phys. Rev. B **45**, 6479 (1992).
- ¹²W.F. Brinkman and T.M. Rice, Phys. Rev. B **2**, 4302 (1970).
- ¹³J. Hubbard, Proc. R. Soc. London, Ser. A **281**, 401 (1964).
- ¹⁴D.E. Logan and P. Nozières, Philos. Trans. R. Soc. London, Ser. A **356**, 249 (1998).
- ¹⁵P. Nozières, Eur. Phys. J. B **6**, 447 (1998).
- ¹⁶S. Kehrein, Phys. Rev. Lett. **81**, 3912 (1998).
- ¹⁷R.M. Noack and F. Gebhard, Phys. Rev. Lett. **82**, 1915 (1999).
- ¹⁸R. Bulla, A.C. Hewson, and T. Pruschke, J. Phys.: Condens. Matter **10**, 8365 (1998).
- ¹⁹R. Bulla, Phys. Rev. Lett. **83**, 136 (1999).
- ²⁰Also for finite temperatures, the IPT results are quantitatively incorrect: Within the IPT the coexistence region $U_{c1} < U < U_{c2}$ shrinks to a single point at a temperature $T_{c, IPT}$ ⁵. Recent QMC calculations by J. Schlipf *et al.*, Phys. Rev. Lett. **82**, 4890 (1999), however, do not show a coexistence of two solutions for temperatures down to at least $0.33T_{c, IPT}$.
- ²¹G. Moeller, Qimiao Si, G. Kotliar, M. Rozenberg, and D.S. Fisher, Phys. Rev. Lett. **74**, 2082 (1995).
- ²²R. Bulla and M. Potthoff, Eur. Phys. J. B (to be published).
- ²³M. Potthoff and W. Nolting, Eur. Phys. J. B **8**, 555 (1999).
- ²⁴L.D. Landau and E.M. Lifshitz, *Statistical Physics* (Pergamon Press, London, 1959).
- ²⁵K. Binder, in *Phase Transitions and Critical Phenomena*, edited by C. Domb and J.L. Lebowitz (Academic, London, 1983), Vol. 8.
- ²⁶N.D. Mermin and H. Wagner, Phys. Rev. Lett. **17**, 1133 (1966).
- ²⁷H. Au-Yang, J. Math. Phys. **14**, 937 (1973).
- ²⁸M. Caffarel and W. Krauth, Phys. Rev. Lett. **72**, 1545 (1994).
- ²⁹M. Potthoff and W. Nolting, Phys. Rev. B **59**, 2549 (1999).
- ³⁰H. Hasegawa, J. Phys.: Condens. Matter **4**, 1047 (1992).
- ³¹G. Kotliar and A. Ruckenstein, Phys. Rev. Lett. **57**, 1362 (1986).
- ³²D.A. Papaconstantopoulos, *Handbook of the Band Structure of Elemental Solids* (Plenum, New York, 1986).
- ³³J. Dorantes-Dávila and G.M. Pastor, Phys. Rev. B **51**, 16 627 (1995).
- ³⁴S. Parhofer, R. Pfandzelter, and M. Potthoff, Phys. Rev. B **53**, 10 377 (1996).
- ³⁵H. Schweitzer and G. Czycholl, Z. Phys. B **83**, 93 (1991).
- ³⁶M. Potthoff and W. Nolting, Z. Phys. B **104**, 265 (1997).
- ³⁷M. Jarrell, Phys. Rev. Lett. **69**, 168 (1992).
- ³⁸J.M. Luttinger and J.C. Ward, Phys. Rev. **118**, 1417 (1960).
- ³⁹A. Georges and W. Krauth, Phys. Rev. B **48**, 7167 (1993).
- ⁴⁰M.J. Rozenberg, G. Kotliar, and X.Y. Zhang, Phys. Rev. B **49**, 10 181 (1994).
- ⁴¹Qimiao Si, M.J. Rozenberg, G. Kotliar, and A.E. Ruckenstein, Phys. Rev. Lett. **72**, 2761 (1994).
- ⁴²M. Rozenberg, G. Moeller, and G. Kotliar, Mod. Phys. Lett. B **8**, 535 (1994).
- ⁴³W.-H. Steeb, *Problems in Theoretical Physics* (BI Wissenschaftsverlag, Mannheim, 1990), Vol. I.
- ⁴⁴E. Müller-Hartmann, Z. Phys. B **74**, 507 (1989).
- ⁴⁵D. Kalkstein and P. Soven, Surf. Sci. **26**, 85 (1971).
- ⁴⁶M.J. Rozenberg, X.Y. Zhang, and G. Kotliar, Phys. Rev. Lett. **69**, 1236 (1992).
- ⁴⁷A. Georges and W. Krauth, Phys. Rev. Lett. **69**, 1240 (1992).
- ⁴⁸R. Haydock, in *Solid State Physics, Advances in Research and Applications*, edited by H. Ehrenreich, F. Seitz, and D. Turnbull (Academic, London, 1980), Vol. 35.
- ⁴⁹R. Haydock and M.J. Kelly, Surf. Sci. **38**, 139 (1973).
- ⁵⁰J.L. Morán-López and J.M. Sanchez, Phys. Rev. B **39**, 9746 (1989).